

GigaScience

Plant phenomics: an overview of image acquisition technologies and image data analysis algorithms --Manuscript Draft--

Manuscript Number:	GIGA-D-17-00043R2	
Full Title:	Plant phenomics: an overview of image acquisition technologies and image data analysis algorithms	
Article Type:	Review	
Funding Information:	Ministerio de Economía y Competitividad (ES) (BFU-2013-45148-R)	Prof.Dr. Marcos Egea-Cortines
	Ministerio de Economía y Competitividad (TIN2012-39279)	Prof Pedro Javier Navarro
	Fundación Séneca (19398/PI/14)	Prof.Dr. Marcos Egea-Cortines
Abstract:	The study of phenomes or phenomics has been a central part of biology. The field of automatic phenotype acquisition technologies based on images has seen an important advance in the last years. As other high throughput technologies, it bears from a common set of problems, including data acquisition and analysis. In this review, we give an overview of the main systems developed to acquire images. We give an in-depth analysis of image processing with its major issues, and the algorithms that are being used or emerging as useful to obtain data out of images in an automatic fashion.	
Corresponding Author:	Marcos Egea-Cortines, PhD Universidad Politecnica de Cartagena Cartagena, Murcia SPAIN	
Corresponding Author Secondary Information:		
Corresponding Author's Institution:	Universidad Politecnica de Cartagena	
Corresponding Author's Secondary Institution:		
First Author:	Fernando Perez-Sanz, MsC	
First Author Secondary Information:		
Order of Authors:	Fernando Perez-Sanz, MsC	
	Pedro Javier Navarro, PhD	
	Marcos Egea-Cortines, PhD	
Order of Authors Secondary Information:		
Response to Reviewers:	<p>Dear Dr. Nogoy,</p> <p>Thanks very much for the opportunity to improve the manuscript. We have met all the requests. We wanted to point out that referee #2 requested a list of advantages and disadvantages for the different types of algorithms used in image analysis. We believe that, while that can be generalized for sensors, it is not the case in image analysis. We argue that the researchers need to test several methods to identify the best for their specific type of image, and forecasting the best outcome is not reasonable. We have written this in the text, and as requested added yet another table. We hope that the work will suffice for publication, waiting of course the verdict of the referees.</p> <p>Bests Marcos</p> <p>Reviewer reports: Reviewer #1:</p>	

I would like to thank the authors for the changes they made in the manuscript. I have the feeling it reads much better now and is more accessible to a broader audience.

I still have a couple of comments/suggestions (minor ones):

Line 49-line 76: I am still not sure to understand why the authors choose to focus this paragraph on the used of gene reporter, which is a very narrow example of the phenotyping today. I would personally remove this section.

We have removed it

Line 581: "The majority of the work has been made in indoor-setups ": I am really not sure about that... A lot of tools and methods have been developed recently to work outdoor and into the field.

We have rephrased it to have a less blunt statement

Reviewer #2: I am appreciated that the authors made big efforts to rewrite this review according to the reviewer's opinions. In recent years, many similar reviews related with Plant Phenomics had been published. And the authors stated that: "a detailed review on different type of data analysis is lacking. In this review, we cover the current and emerging methods of image acquisition and processing allowing image-based phenomics". This review should focus on image data analysis depending on different data type or sensors, which is lacking. Thus, two major issues should be improved and summarized more clearly in this review. Moreover, some previous comments are ignored by the authors or the related sentences had been removed, which should be declared.

We took into consideration all the previous comments, but as we made a major rewriting, they do not always appear as a word by word answer.

From the previous version:

"We have corrected this (line 222)

17.Line 160-163: please add references.

18.Line 167-169: please add references.

19.Line 173-177: please add references.

20.Line 178-181: More applications of plant phenotyping with LIDAR in recent years should be cited. Please discuss the disadvantage of the LIDAR.

21.Line 177: the end of the sentence lacks punctuation.

We have rewritten this whole part and included new references

22.Line 186: "14.000 nm" should be change to "14,000 nm". The image which obtained by thermographic camera should include a range of wavelength. Moreover, please add the reference.

We have added the reference. We have added fluorescence imaging with the corresponding ranges and references (line 297-322)

23.Line 196: "as a result of UV light excitation" is not rigorous, and please add the reference.

We have rewritten this part (see above line 397-322)

24.Line 75-203: more image acquisition techniques, such as x-ray CT, should be added. And the authors should summarize the merit and drawback of these imaging techniques.

25.Line 227-229: please add the reference of the "In fact, when information is measured as entropy, pre-processing causes a decrease in entropy". Or this is the author's own opinion.

We have rewritten this entire section

26.Line 235-265: please introduce the procedures of image correction and images enhancement more concisely, and please add the reference.

We have rewritten this entire section

27.Line 271-272: please add the references to the "Leaf Area Index (LAI), biomass,

chlorophyll concentration, photosynthetic activity", respectively.
28.Line 287: please add the references to the "RDVI" and "MSR".
29.Line 294: what "NIR" and "VIS" represented?
30.Line 301: "EVI (enhanced vegetation index)" should be changed into "enhanced vegetation index (EVI)". Please check the similar mistake carefully in the main text.
31.Line 305: you should add the meaning of "RED" and "BLUE".
32.Line 267-312: the summarization of indexes in Table 1 is appreciated. But the "Vegetation indexes" part may not be appropriate for the "Image pre-processing" part, and this part is too redundant.
33.Line 320: 3D or 3-D.
34.Line 336-337: please add the references of the "1500-1590 nm" and "1390-1430 nm".
35.Line 355: Despite RGB and HSV colour space, other colour components such as ExG are also frequently used in plant detection. The authors should introduce more colour components.
36.Line 359-360: please add the references of the "hue can discriminate to detect chlorophyll".
37.Line 368: what is the meaning of "h(.)"?
38.Line 394: please add the references of the "Gaussian Mixture Model (GMM)". And what is the meaning of "l"?
39.Line 474: what are the meaning of "(892-934)" and "(281-245)"?
40.Line 476: 28 in SURF?
41.Line 487: please use the full name of "FAST" for the first time.
42.Line 442-517: The authors give too much detail about the features. Little was introduced about the application of these features in plant phenotyping.
43.Line 538-544: The authors should give some suggestion about when to select supervised/unsupervised techniques.
44.Line 545-547: I agree that the selection of ML algorithm require actual experimentation for optimal results. However, there are some general advices, the author should mention that and give some suggestions.

We have rewritten this part to make it more accessible. As a result, all the comments have been taken into account
“

As you can see, the major rewriting does take into account your ideas and suggestions.

1.The authors should summarize the imaging techniques in one table, which includes sensors, applications, advantages, disadvantages, and so on.

The authors could find a good example in Table 1 of the reference: "44. Fiorani F, Schurr U. Future scenarios for plant phenotyping. Annu. Rev. Plant Biol."

-We wrote a table as suggested. Please notice that the table is empty on the algorithms of machine learning and ToF. As of today there isn't a single paper published applied to phenomics.

The aforementioned table does describe advantages and disadvantages of sensors(Fiorani and Schurr). However, during image analysis, the advantages or disadvantages are a case by case situation. Researchers end up using the procedure giving better results for the specific image acquisition setup.

The complex combinations of background, reflected image, wavelength, sensors and the rest of elements that comprise image acquisition, makes it impossible to come with a single recipe for image analysis. The current review tries to give a number of methods for the different stages of image processing. But it will always be the researcher the one to test the different approaches to identify the combinations that give better results.

So it would be misleading to write for instance that a SIFT algorithm will have advantages over RGB2Grayscale for stereo vision (see new table 4), as it will depend

on the image, background, type of plant, etc.

The fact that there are so many publications testing different methods and algorithms shows that image analysis is very much a trial and error procedure till a defined pipeline is setup for a specific need. We think this message has to get through.

2. In image analysis section, the structure should be re-organized and more sub-sections should be added. For example in image pre-processing section, the review should provide different strategies according to different sensors or data types (such as CT raw data, hyperspectral raw data, RGB raw data, infrared raw data, and so on). We disagree with this as once an image is taken, the downstream process does not depend on the type of sensor used. We made table 4 to show what has been done so far, as requested. But once you have a matrix of pixels, the rest should be common procedures.

We have included a comprehensive table (Table 4) has been included as requested

Line 574:
A summary of the complete pipeline of image analysis including sensors, preprocessing, segmentation procedures, feature extractions and machine learning algorithms can be found in Table 4.

I believe that different imaging data need different pre-processing strategies. The authors just reviewed many pre-processing methods, but why choose this method and how to apply is lacking.

-As we said before this is incorrect, an image is a matrix of pixels. Authors test several methods and report the one that gave the best results.

The authors stated that: "We cannot conclude that a single preprocessing method will outperform other methods". Thus, the better or common used preprocessing method to handle different images is needed and should be listed in one table, which can benefit broader readers. The similar suggestions of the section "image segmentation, feature extraction" should be considered to modify this review.

We have added on table 4 a list of the most common used procedures. How to apply the different methods is a matter of taking the raw data and using different procedures and see for EACH case what gives better results. As we wrote above, recommending one over the other would be misleading. Furthermore, the current list of methods will probably increase in the future as the number of labs doing image analysis has increased dramatically in the last years.

Additional Information:	
Question	Response
Are you submitting this manuscript to a special series or article collection?	No
Experimental design and statistics	No
Full details of the experimental design and statistical methods used should be given in the Methods section, as detailed in our Minimum Standards Reporting Checklist . Information essential to interpreting the data presented should be made available in the figure legends.	
Have you included all the information requested in your manuscript?	

<p>If not, please give reasons for any omissions below.</p> <p>as follow-up to "Experimental design and statistics</p> <p>Full details of the experimental design and statistical methods used should be given in the Methods section, as detailed in our Minimum Standards Reporting Checklist. Information essential to interpreting the data presented should be made available in the figure legends.</p> <p>Have you included all the information requested in your manuscript?</p> <p>"</p>	<p>Not aplicable</p>
<p>Resources</p> <p>A description of all resources used, including antibodies, cell lines, animals and software tools, with enough information to allow them to be uniquely identified, should be included in the Methods section. Authors are strongly encouraged to cite Research Resource Identifiers (RRIDs) for antibodies, model organisms and tools, where possible.</p> <p>Have you included the information requested as detailed in our Minimum Standards Reporting Checklist?</p>	<p>Yes</p>
<p>Availability of data and materials</p> <p>All datasets and code on which the conclusions of the paper rely must be either included in your submission or deposited in publicly available repositories (where available and ethically appropriate), referencing such data using a unique identifier in the references and in the "Availability of Data and Materials" section of your manuscript.</p> <p>Have you have met the above requirement as detailed in our Minimum Standards Reporting Checklist?</p>	<p>Yes</p>

1 **Gigascience Review**

2

3 **Plant phenomics: an overview of image acquisition technologies and**
4 **image data analysis algorithms**

5 Fernando Perez-Sanz¹, Pedro J. Navarro², Marcos Egea-Cortines²

6

7

8 ¹Genetics, ETSIA, Instituto de Biotecnología Vegetal, Universidad Politécnica de

9 Cartagena, 30202 Cartagena, Spain

10 ²DSIE, Universidad Politécnica de Cartagena, Campus Muralla del Mar, s/n. Cartagena

11 30202, Spain

12 email- Fernando Perez-Sanz- fernando.perez8@um.es; Pedro J. Navarro

13 pedroj.navarro@upct.es

14 Correspondence Marcos Egea-Cortines marcos.egea@upct.es

15

16

17 Abstract

18

19 The study of phenomes or phenomics has been a central part of biology. The field of
20 automatic phenotype acquisition technologies based on images has seen an important
21 advance in the last years. As other high throughput technologies, it bears from a
22 common set of problems, including data acquisition and analysis. In this review, we
23 give an overview of the main systems developed to acquire images. We give an in-depth
24 analysis of image processing with its major issues, and the algorithms that are being
25 used or emerging as useful to obtain data out of images in an automatic fashion.

26

27 **Keywords:** algorithms; artificial vision; deep learning; hyperspectral cameras; machine
28 learning; segmentation

29 Background

30

31 The development of systems to monitor large fields using Normalized Difference
32 Vegetation Index (NDVI), started a long successful career over 25 years ago when
33 NDVI was used in the so-called remote sensing field [1]. It was an important milestone
34 in the advance of automatic methods for analysing plant growth and biomass [2]. Ever
35 since, new technologies have increased our capacity to obtain data from biological
36 systems. The ability to measure chlorophyll status from satellite images allowed plant
37 health to be measured in large fields and predict crops and productivity in very large
38 areas such as the Canadian prairies, Burkina Faso or the Indian Basin in Pakistan [3–6].
39 Thus, the field of remote sensing is an important basis where knowledge about data
40 acquisition and analysis started. The development of phenotyping devices using local
41 cameras for crops took off using an array of technologies including Infrared
42 thermography to measure stomatal opening or osmotic stress [7–9]. Extraction of
43 quantitative data from images has been developed to study root development [10–12],
44 and has found a niche to identify germplasm resistant to abiotic stresses in plants such
45 as cereals [13], Arabidopsis [14] and for large-scale field phenotyping [15]. There are
46 several recent reviews addressing the different types of growing setups [16–22], and we
47 will not cover them in the current review.

48

49

1
2
3
4
5
6
7
8
9
10
11
12
13
14
15
16
17
18
19
20
21
22
23
24
25
26
27
28
29
30
31
32
33
34
35
36
37
38
39
40
41
42
43
44
45
46
47
48
49
50
51
52
53
54
55
56
57
58
59
60
61
62
63
64
65
66
67
68
69
70
71
72
73
74
75
76
77
78
79
80
81
82

Two main aspects to consider are the type of image acquired and how to process it. There are a number of recent reviews on phenomics and high-throughput image data acquisition [15,23–26]. In contrast, the majority of the literature concerning image processing and analysis is found in books where methods are described in detail [27–31]. There are some very good reviews on aspects of data acquisition and analysis i.e. imaging techniques [32], Machine Learning (ML) for high throughput phenotyping [33] or software for image analysis [34], but a detailed review on different type of data analysis is lacking. In this review, we cover the current and emerging methods of image acquisition and processing allowing image-based phenomics (Figure 1).

Review

Image acquisition

Image acquisition is the process through which we obtain a digital representation of a scene. This representation is known as image and its elements are called pixels (picture elements). The electronic device used to capture a scene is known as imaging sensor. CCD (charge-coupled device) and CMOS (complementary metal oxide semiconductor) are the most broadly used technologies in image sensors. A light wavelength is captured by small analogic sensors, which will acquire major or minor charge depending on the amount of incident light. These signals are amplified, filtered, transported and enhanced by means of specific hardware. A suitable output interface and a lens in the same housing is all that it is needed to perform image acquisition. The elements enumerated above conform the main element of computer vision systems, the camera. Time delay and integration (TDI) is an imaging acquisition mode that can be implemented over CCD [35] or CMOS [36]. It improves the features of the image acquisition system considerably. TDI is used in applications that require the ability to operate in extreme lighting conditions, requiring both high speed and high sensitivity, for example: inline monitoring, inspection, sorting, and remote sensing (for weather o vegetation observation) [36].

The aforementioned technologies, CCD, CMOS and TDI confer unique characteristics, which define the type of data a camera can provide with a degree of robustness. There are fundamental differences in the type of performance the different sensors offer. In the last years CMOS technology, has outperformed CCDs in most visible imaging

1
2
3
4
5
6
7
8
9
10
11
12
13
14
15
16
17
18
19
20
21
22
23
24
25
26
27
28
29
30
31
32
33
34
35
36
37
38
39
40
41
42
43
44
45
46
47
48
49
50
51
52
53
54
55
56
57
58
59
60
61
62
63
64
65

83 applications. When selecting an imaging sensor (a camera), CCD technology causes less
84 noise and produces higher quality images, mainly in scenes with bad illumination. They
85 have a better depth of colour due to their higher dynamic range. On the other hand, the
86 CMOS sensors are faster at processing images. Due to the hardware architecture for
87 pixel extraction, they need less electrical power to operate, they allow a Region of
88 Interest (ROI) to be processed on the device and are cheaper than CCDs. Furthermore,
89 TDI mode with CCD or CMOS imaging sensors is used for high speed and low light
90 level applications [37]. The latest technological developments in cameras show that the
91 trend of the manufacturers such as IMEC, world-leader in nanoelectronics, is to fuse
92 TDI technology with the CCD and CMOS characteristics in the same device [38]. TDI
93 technology is expected to be applied to high throughput phenotyping processes in the
94 nearby future.

95

96 The field of image acquisition is extremely developed with considerable literature but
97 image acquisition systems can be classified into seven groups that are suitable for
98 phenotyping.

99

100 1. Mono-RGB vision

101

102 Mono-RGB vision systems are composed of a set comprising a lens, imaging sensor,
103 specific hardware and IO interface. Depending if they use a line or matrix of pixels,
104 they are classified in line cameras (or scanners) and matrix cameras. Most computer
105 vision phenotyping devices are based on mono-RGB vision systems. Examples of
106 mono-RGB vision devices include “Smart tools for Prediction and Improvement of
107 Crop Yield (SPICY)”, an automated phenotyping prototype of large pepper plants in the
108 greenhouse. The system uses multiple RGB cameras to extract two types of features:
109 features from a 3D reconstruction of the plant canopy and statistical features derived
110 directly from RGB images [39]. A different approach has been used with two cameras
111 inside a growth chamber to measure circadian growth features of *Petunia*, *Antirrhinum*
112 and *Opuntia* [40]. Two cameras with low and high magnifications were used to carry-
113 out phenotype studies of *Arabidopsis thaliana* seeds. The system is mounted on a three-
114 axis gantry and the rotation of the samples allow the gravitropic bending response to be
115 determined in the roots and its posterior quantification [41]. Recently a high-throughput
116 RGB system has been developed to identify Quantitative Trait Loci (QTL) involved in

117 yield in large recombinant inbred lines in maize [42], demonstrating the increasing
118 impact of this approach in phenomics.

119 These devices have excellent spatial and temporal resolution, i.e. they can produce a
120 very large number of images in very short periods and at a very low cost. They are
121 portable and there are many software tools to perform image processing (Table 1).
122 Systems based on mono-RGB vision allow a quantification of the plant canopy [43], as
123 well as sufficient computation of vegetation indices, for most purposes. The main
124 disadvantages are caused by the overlap of plant organs during growth and nutation
125 phases and the relative position of the organs with respect to the device that makes the
126 precise quantification difficult. In addition, these devices are affected by variations in
127 illumination when used outdoors. The trend in outdoor plant phenotyping is to combine
128 mono-RGB systems with other systems such as Light Detection and Ranging LIDAR
129 devices (see below), thermal imaging or adding new bands or filters to the camera that
130 allow the segmenting of specific regions of the spectrum [44,45].

131

132 2. Stereo vision

133

134 Stereo vision systems try to correct a drawback of mono-RGB vision systems for
135 distance measurement. The architecture of stereo vision systems emulates the behaviour
136 of human vision using two mono vision systems. Basically, and after locating a point in
137 two mono vision systems, it is possible to compute the distance from the point to the
138 system. Images produced are known as depth maps [46]. A stereo vision system has
139 been used by Biskup and colleagues [47] to obtain structural features of plant canopies.
140 The 3D reconstruction has been successfully employed to obtain 3-D models of plants,
141 thus demonstrating the power of this approach [48]. Simple depth reconstructions
142 helped to define stems, leaves and grapes showing the potential of this technology [49].
143 A RGB camera mounted on a mobile robot is used as an automated 3D phenotyping of
144 vineyards under field conditions. Sequentially, the system captures a set of images,
145 which are used to reconstruct a textured 3D point cloud of the whole grapevine row
146 [50]. A stereo vision has been developed to perform high throughput analysis of
147 rapeseed leaf traits. The system uses two identical RGB cameras to obtain stereo images
148 for canopy and 3-D reconstruction [51]. Developing a 3D-mesh segmentation has
149 allowed cotton growth to be analysed [52], showing the further possibilities of 3D
150 imaging.

151

152 The main advantage of 3-D systems is their simplicity, two cameras are enough to
153 obtain depth maps. The stereo vision has evolved in multi-view stereo (MSV) and has
154 found a place in plant phenotyping [53]. Furthermore, the MSV is a low cost 3D image
155 acquisition system compared with other technologies such as LIDAR or tomography
156 imaging [54]. Stereo vision systems have important weaknesses. They are affected by
157 changes of the scene illumination, they need a high performance computational system
158 to carry out stereo matching algorithms, and they have a poor depth resolution [55].
159 These limitations are increased in outdoor environments, as image segmentation
160 becomes more challenging.

161

162 3. Multi and hyper spectral cameras

163

164 The multispectral and hyperspectral cameras have been used in numerous fields of
165 science and in industrial applications [56–61]. The spectral resolution is the main factor
166 that distinguishes multispectral imagery from hyperspectral imagery [62]. Multispectral
167 cameras are devices able to capture images from a number of discrete spectral bands.
168 The number of bands has increased in the last decade as technology has improved.
169 Currently, the main camera manufacturers offer multispectral cameras acquiring
170 between three and twenty five bands, including the visible RGB channels, Near Infra-
171 Red (NIR) or a set of custom bands, with a tendency to provide increasing number of
172 bands [63]. The spectral bands may not be continuous, thus for one pixel we obtain a
173 vector of information comprising the number of elements corresponding to the number
174 of bands registered. Hyperspectral systems may reach resolutions of a few nanometers
175 in wavelength, obtaining for each pixel a digital signature that may contain several
176 hundreds of continuous bands within a specific range of wavelengths [64].
177 Traditionally, both multispectral and hyperspectral imaging have been used for remote
178 sensing and have an increased number of applications in phenomics. A multispectral
179 system has been developed to improve the original colour of images for fruit
180 recognition [65]. The authors fused the original colour image with an infrared image
181 using the nonlinear Daubechies wavelet transform (DWT). Thus, the additional
182 information from a second image allows the original one to be improved.

183

184 The use of hyperspectral cameras is increasing in phenotyping experiments as they
185 allow the identification of physiological responses, pathologies or pests in a non-
186 invasive way. Using hyperspectral images, a system has been developed to identify
187 pathogens in barley leaves using probabilistic topic models [66]. A hyperspectral
188 microscope was used to determine spectral changes on the leaf and cellular level of
189 barley (*Hordeum vulgare*) during resistance reactions against powdery mildew
190 (*Blumeria graminis f.sp. hordei*, isolate K1) [67]. A detailed description of the different
191 wavelengths and combinations used in multispectral and hyperspectral cameras can be
192 seen in Figure 2, and their uses in Table 2. We expect to see an increase in phenomic
193 setups using multispectral and hyperspectral cameras in the future. An emerging issue
194 will be the data analysis as the number of pictures doubles with each additional
195 spectrum used for analysis (see below).

196

197 4. ToF cameras

198

199 The Time of Flight cameras or ToF cameras have been one of the last imaging devices
200 to be incorporated into automatic plant phenotyping [68]. ToF has as a general principle
201 the measurement of the distance between the objective of the camera and each pixel.
202 This is achieved measuring the time it takes for a signal emitted in NIR to come back,
203 reflected by the object. This allows a precision 3D reconstruction. Stereo vision coupled
204 with ToF images have been implemented to increase the performance of methods of
205 image segmentation to obtain leaf areas [69]. Beyond the tedious hand work required
206 for manual analysis sampling is done in a non-destructive way. Depth maps obtained by
207 a ToF camera together with colour images are used to carry out the 3D modelling of
208 leaves. The system is mounted on a robotic arm which allows image acquisition to be
209 automated [70]. A ToF has been successfully used to identify QTL regulating shoot
210 architectures of *Sorghum* by mean of 3D reconstruction [71].

211 Microsoft Kinect is a low cost image acquisition system designed for video gaming
212 which can be used for characterization and for tracking of phenological parameters [72].
213 The device is composed of an infrared projector and camera that generates a grid from
214 which the location of a nearby object in 3 dimensions can be ascertained [73]. Kinect
215 has been used to measure plant structure and size for two species growing in California
216 grassland [74]. The quantitative 3D measurements of the architecture of the shoot and

1 217 structure of the leaves can be performed when proper segmentation algorithms are
2 218 developed suggesting some potential for ToF systems [75].
3 219
4
5 220 The main disadvantages of this acquisition system are the low resolution, a reduced
6 221 distance range of a few meters and the high dependence on the reflecting surface for
7 222 imaging. As a result, they cannot operate under strong sunlight and are more appropriate
8 223 for indoor conditions. Its reduced cost and the possibility of obtaining 3D structures of
9 224 entire plants, as well as of individual organs make these devices very attractive for
10 225 indoor phenotyping.
11
12
13
14
15
16 226
17
18 227 5. LIDAR technology
19 228
20
21 229 Light Detection and Ranging (LIDAR) is a remote sensing technology developed at the
22 230 beginning of the 70s to monitor the Earth's Surface [76]. LIDAR uses a laser pulse light
23 231 to measure the distance between the light source and the object by calculating the time
24 232 of emission and time of reflected light detection. It allows the creation of a cloud of
25 233 points that reconstruct the 3D structure of an object [77,78]. LIDAR has been used in
26 234 image acquisition from distances of thousands of kilometres to centimetres,
27 235 demonstrating the great potential of these type of devices. Satellite-based LIDAR
28 236 systems are used for the measurements of vegetation canopy height, area, volume or
29 237 biomass, etc. [79–81]. Recent development using both manned and unmanned flights
30 238 have allowed the estimation of biomass dynamics of a coniferous forest using Landsat
31 239 satellite images together with ground and airborne LIDAR measurements
32 240 [82]. Terrestrial LIDAR sensors are applied to detect and discriminate maize plants and
33 241 weeds from soil surface [83]. Short range LIDAR can be deployed for high-throughput
34 242 phenotyping (HTP) systems for cotton plant phenotyping in the field [84] or tomato leaf
35 243 area by 3-D laser reconstruction [85]. Fully automated crop monitoring is feasible using
36 244 centimetre ranges from robotized or gantry systems [43]. An autonomous robotic
37 245 system has allowed 3D mapping of plant structures to be performed with millimetric
38 246 precision [86]. A LASER SCAN mounted on a XYZ gantry system was used to
39 247 estimate the growth measures and structural information of plants through laser
40 248 triangulation techniques [87]. Thus, using different devices LIDAR has an impressive
41 249 range of possibilities for plant phenomics.
42
43
44
45
46
47
48
49
50
51
52
53
54
55
56
57
58
59
60 250
61
62
63
64
65

1
2
3
4
5
6
7
8
9
10
11
12
13
14
15
16
17
18
19
20
21
22
23
24
25
26
27
28
29
30
31
32
33
34
35
36
37
38
39
40
41
42
43
44
45
46
47
48
49
50
51
52
53
54
55
56
57
58
59
60
61
62
63
64
65

251 Some shortcomings of LIDAR devices for plant phenotyping are the absence of colour
252 in the measurement, excessive time to compute the cloud points, low precision for
253 massive phenotyping, scanning noises caused by wind, rain, insects, small particles in
254 the air, and the requirement of calibration. Recent advantages suggest that the use of
255 LIDAR technologies could overcome some of challenges for the next-generation
256 phenotyping technologies [88]. Developments in multispectral LIDAR instruments
257 show novel systems which are capable of measuring multiple wavelengths and of
258 obtaining vegetation indexes (see below) [89,90] or to measure arboreal parameters
259 [91]. The massive adoption of LASER technologies by autonomous car manufactures
260 has fostered the development of 3D High Definition LIDAR (HDL) with real time (RT)
261 capacities. The new 3D HDLs are capable of generating 1.3 million points per second
262 with precisions of 2 cm and distances of up to 120 meters [92]. These new devices open
263 the door to the RT massive phenotyping in outdoor and indoor crops.

264

265 6. Thermography and Fluorescence Imaging

266

267 Thermography is a widely-used technology in remote sensing and plant phenotyping
268 [93–96]. Thermographic cameras are able to acquire images at wavelengths ranging
269 from 300 to 14,000nm [97], thus allowing the conversion of the irradiated energy into
270 temperature values, once the environmental temperature is assessed. Plants open
271 stomata in response to environmental cues and circadian clock depending on the type of
272 photosynthetic metabolism they have [98,99]. The evapotranspiration can be assessed
273 with thermography [100], and quantification can be made at different scales such as a
274 leaf, a tree, a field or a complete region. Water stress and irrigation management are two
275 fields of application of thermography imaging [101–104]. Thermography imaging can
276 detect local changes of temperature produced due to pathogen infection or defence
277 mechanisms [105]. *Oerke et al.* used a digital infrared thermography to correlate the
278 maximum temperature difference (MTD) of apple leaves with all stages of scab
279 development [106].

280

281 Fluorescence imaging has been used in a large number of experimental setups as UV
282 light in the range of 340-360 nm is reflected by different plant components as discrete
283 wavelengths [32]. The corresponding wavelengths emitted are cinnamic acids in the
284 range of green-blue (440-520 nm). Early experiments using reflected fluorescence

285 allowed the identification of phenylpropanoid synthesis mutants in Arabidopsis [107].
286 Chlorophyll fluorescence emits in red and far-red (690-740 nm). It is an important
287 parameter that has been studied as a proxy for different biological processes such as
288 circadian clock or plant health [8,108,109]. A system based on a UV light lamp and a
289 conventional camera provided of a UV-filter to avoid RGB and IR images has been
290 used to identify changes in UV absorbance related to pollination [110]. Multicolour
291 fluorescence detection uses the combination of chlorophyll and secondary metabolites
292 emitted fluorescence to determine plant health in leaf tissues [111].

293

294 Thermography imaging results in an estimable tool for monitoring of genotypes and
295 detection of plant diseases [112] where all the specimens are located under strict control
296 conditions: temperature, wind velocity, irradiance, leaf angle or canopy leaf structures
297 are potential issues for quality image acquisition. The next generation of thermography
298 imaging for phenotyping will have to resolve drawbacks related to temporal variations
299 of environment conditions, aspects relating to angles of view, distance, sensitivity and
300 reproducibility of the measurements [104]. Both thermographic and fluorescent images
301 capture a single component and images are in principle easy to analyse as segmentation
302 based on thresholds can be applied to the acquired images. Combining thermographic
303 and fluorescent imaging requires sophisticated data analysis methods based on neural
304 networks to obtain quality data but are an emerging solution [111].

305

306 7. Tomography imaging

307

308 Magnetic Resonance Imaging (MRI) is a non-invasive imaging technique which uses
309 Radio Frequency (RF) magnetic fields to construct tomographic images [113].
310 Commonly MRI has been used to investigate the anatomy structure of the body
311 (especially the brain) in both health and disease [114]. In plant phenomics, MRI is used
312 to visualize internal structures and metabolites. This method poses a great potential to
313 monitor physiological processes occurring *in vivo* [115]. MRI has allowed the
314 development of root systems over time in bean to be mapped [116], moisture
315 distribution to be visualized during development in rice [117] and the water presence to
316 be analysed during maturity process of barley grains [118].

317 Positron Emission Tomography (PET) is a nuclear medicine imaging modality that
318 allows the assessment of biochemical processes *in vivo*, to diagnose and stage diseases

319 and monitor their treatment [119]. *Karve et al.* [120] presented a study about C-
320 allocation (Carbon allocation from CO₂ through photosynthesis) in large grasses such as
321 *Sorghum bicolor*. The study concluded that the commercial PET scanners can be used
322 reliably, not only to measure C-allocation in plants but also to study dynamics in
323 photoassimilate transport.

324
325 X-ray Computed Tomography (X-ray CT) employs X-rays to produce tomographic
326 images of specific areas of the scanned object. The process of attenuation of rays
327 together with a rotation and axial movement over objects produces 3D images [32]. A
328 high throughput phenotyping system based on X-ray CT is ten times more efficient than
329 human operators, being capable of detecting a single tiller mutant among thousands of
330 rice plants [121]. The remarkable penetration of X-rays, has made this technology a
331 great ally of phenotyping carried out below-ground. The study of root systems and their
332 quantification has been a field of habitual application of X-ray CT [122–126]. New
333 developments address the reduction of penetrability and the increase of the image
334 resolution of X-ray CT in plant tissue using phosphotungstate as a contrasting agent,
335 due to its capacity of increasing the contrast and penetrability of thick samples [127].

336
337 MRI, PET and X-ray imaging techniques are available for screening 3-D objects. MRI
338 and PET are two non-destructive and non-invasive scanning technologies that have been
339 applied in plant sciences to acquire 3-D structural information [128]. MRI and PET data
340 acquisition is time consuming, and software tools need to be further developed to
341 analyse data and obtain physiologically interpretable results [97]. High-Resolution X-
342 ray computed tomography (HRXCT) promises to be the broadest non-destructive
343 imaging method used in plant sciences. HRXCT will provide 3-D data at a resolution
344 suited for detailed analysis of morphological traits of *in vivo* plant samples and at a
345 cellular resolution for *ex vivo* samples [128]. From of a point of view of the devices the
346 trend will be to increase the resolution of images, the size of the fields of view, and
347 increase its portability [129].

348

349 Image analysis

350

351 Extracting information from images is performed through the process of segmentation.
352 The aim of a segmentation procedure is to extract the components of an image that are
353 of interest i.e. object or region of interest from the rest of the image i.e. background of
354 the image or irrelevant components. Thus, we end up with a partitioned image with
355 significant regions. The significant regions may be defined as foreground versus
356 background, or by selecting a number of individual components from an image. The
357 construction of the selected regions is based on the image characteristics such as colour
358 (colour spaces), spectral radiance (vegetation indexes), edge detection, neighbour
359 similarity [130] or combinations that are integrated via a machine learning process
360 [131]. In some cases, pre-processing is required in order to obtain a meaningful
361 segmentation.

362

363

364 1. Image pre-processing

365

366 Image preprocessing is an important aspect of image analysis. The aim of image
367 preprocessing is to improve contrast and eliminate noise in order to enhance the objects
368 of interest in a given image [132]. This process can be extremely helpful to enhance the
369 feature extraction quality and the downstream image analysis [133]. Preprocessing can
370 include simple operations such as image cropping, contrast improvement or others
371 significantly more complex such as dimensionality reduction via Principal Component
372 Analysis or Clustering [33]. One preprocessing pipeline has been proposed for plant
373 phenotyping based on converting the image to grayscale, application of a median filter,
374 binarization and edge detection [134]. A similar preprocessing has been developed to
375 identify plant species under varying illumination conditions [135]. It comprises
376 conversion to grayscale, image binarization, smoothing and application of a filter to
377 detect edges. In a comparative study to analyze leaf diseases, histogram equalization
378 was found to be the best way to obtain preprocessing of color images converted to
379 grayscale [136]. However RGB images have been found to perform better than
380 grayscale conversions when identifying leaf pathogens [137].

381

382 We cannot conclude that a single preprocessing method will outperform other methods.
383 The quality and type of image are fundamental to select a type of preprocessing
384 procedure. Nevertheless, preprocessing is a basic step that can improve image analysis,

385 and sometimes make it possible. It should be described in the materials and methods
386 of image procedures to make data comply the new standards -Findability, Accessibility,
387 Interoperability, and Reusability (FAIR) [138]

388

389 2. Image segmentation

390

391 As we mentioned above, image segmentation is the core of image processing for
392 artificial vision-based plant phenotyping. Segmentation allows the isolation and
393 identification of objects of interest from an image, and it aims to discriminate
394 background or irrelevant objects [139]. The objects of interest are defined by the
395 internal similarity of pixels in parameters such as texture, colour, statistic [133], etc.
396 (See a list of Open software libraries for image segmentation in Table 1).

397

398 One of the simplest algorithms used is threshold segmentation, based on creating groups
399 of pixels on a grayscale according to the level of intensity, thus separating the
400 background from targets. Such an approach has been used with Android OS (ApLeaf) in
401 order to identify plant leaves [140].

402

403 The Otsu's method [141] is a segmentation algorithm that searches for a threshold that
404 minimizes the weighted within class variance [132]. This method has been used for
405 background subtraction in a system that records and performs automatic plant
406 recognition [142], and can give high contrast segmented images in an automatic fashion
407 [143]. Under certain circumstances, it can underestimate the signal causing under
408 segmentation, and is significantly slower than other thresholding methods [132].

409

410 The Watershed [144] transformation is a popular algorithm for segmentation. It treats an
411 image as a topological surface that is flooded, and seed regions are included, usually by
412 the user. This generates an image with gradients of magnitudes, where crests appear in
413 places where borders are apparent (strong edges), and causes segmentation to stop at
414 those points [130]. It has been used to identify growth rate [145], recognition of
415 partially occluded leaves [56], individual tree crown delineation [146] or leaf
416 segmentation [147].

417

1
2
3
4
5
6
7
8
9
10
11
12
13
14
15
16
17
18
19
20
21
22
23
24
25
26
27
28
29
30
31
32
33
34
35
36
37
38
39
40
41
42
43
44
45
46
47
48
49
50
51
52
53
54
55
56
57
58
59
60
61
62
63
64
65

418 Grabcut [148] is a segmentation algorithm based on graph cut [149]. It is created on
419 graph theory to tackle the problem of separating an object or foreground from the
420 background. The user should mark a rectangle (bounding box) surrounding the object of
421 interest thus defining the outrebound of the box as background [150]. This algorithm
422 has been tested to extract trees from a figure but it has been successful only with very
423 simple backgrounds [151]. More recently Grabcut has been deployed as a segmentation
424 algorithm in a pipeline for plant recognition with multimodal information i.e. leaf
425 contour, flower contour etc [152]. Grabcut loses precision or even fails when pictures
426 have complex backgrounds but is highly precise with simple backgrounds [151,153].

427
428 Snakes are a special type of active contour [154], and are used as methods to fit lines
429 (splines) either to open or close edges and lines in an image. These methods have been
430 used for face recognition, iris segmentation and medical image analysis. Within the
431 field of plant phenotyping, there are procedures where active contours are used inside a
432 protocol constructing a vector of features with data of colour intensity, local texture and
433 a previous knowledge of the plant incorporated via Gaussian Mixture Models,
434 previously segmented [155] . These steps give an initial rough segmentation upon
435 which, active contours can operate with a much higher precision.

436
437 Active contours have used for plant recognition via images of flowers [156], based on a
438 combination of the algorithm proposed by Yonggang and Karl [157] and the model of
439 active contours without edges [158]. Whilst the work proposed by Minervini et al [155]
440 appears to give significantly better results compared to those of Suta et al [156], the
441 usage of images with a natural background maybe related to the apparent differences in
442 segmentation. Thus, a current problem concerning the comparison of algorithms and
443 procedures lies on the different backgrounds used for image acquisition.

444 445 3. Features extraction

446
447 Features extraction constitutes one of the pillars of the identification and classification
448 of objects based on computer vision. Beyond the raw image, a feature is information
449 which is used to resolve a specific computer vision problem. The features extracted
450 from an image are disposed in the so-called “feature vectors”. The construction of
451 feature vectors uses a wide set of methods to identify the objects in an image. The main

1
2
3
4
5
6
7
8
9
10
11
12
13
14
15
16
17
18
19
20
21
22
23
24
25
26
27
28
29
30
31
32
33
34
35
36
37
38
39
40
41
42
43
44
45
46
47
48
49
50
51
52
53
54
55
56
57
58
59
60
61
62
63
64
65

452 features are edges, intensity of image pixels [39], geometries [159], textures [155,160],
453 image transformations e.g. Fourier [161], or Wavelet [65,162] or combinations of pixels
454 of different colour spaces [131]. The end goal of feature extraction is to feed up a set of
455 classifiers and machine learning algorithms (see below).

456
457 One system proposed uses a feature vector composed of a combination of RGB and CIE
458 L*a*b* colour spaces to segment the images captured during the day [131]. The night-
459 time image segmentation computed a vector composed of statistical features over two
460 decomposition levels of the wavelet transform using IR images.

461 Iyer-Pascuzzi et al. presented an imaging and analysis platform for automatic
462 phenotyping to identify genes underlying root system architecture. The authors
463 employed a set of 16 statistical, geometrics and shape features obtained from 2,297
464 images from 118 individuals such as median and maximum number of roots, the total
465 root length, perimeter, depth, among others [163].

466
467 There are a number of algorithms to identify invariant features detectors and
468 descriptors. This type of image analysis ensures the detection of points of interest in a
469 scale and rotation independent manner. This is crucial for camera calibration and for
470 matching to produce a set of corresponding image points in 3D image reconstruction.
471 Furthermore, it allows the identification of points of interest even when they change
472 scale and/or position or situations of uncontrolled illumination, a common issue when
473 phenotyping plants. The Scale Invariant Features Transforms (SIFT) [164], Speeded-Up
474 Robust Features (SURF) [165] and the Histograms of Oriented Gradients (HoG) [166]
475 are algorithms used to extract characteristics in computer vision and they have been
476 extended to plant phenotyping. Wei et al. [167] presented an image-based method that
477 automatically detects the flowering of paddy rice. The method uses a scale-invariant
478 feature transform descriptor, bag of visual words, and a machine learning method. The
479 SIFT algorithm has been used to combine stereo and ToF images with automatic plant
480 phenotyping. It can create dense depth maps to identify pepper leaf in glasshouses [69].
481 SIFT and SURF algorithms have been tested for detecting local invariant features for
482 obtaining a 3D plant model from a multi-view stereo images [168]. A HoG framework
483 allows the extraction of a reliable quantity of phenotypic data of grapevine berry using a
484 feature vector composed of colour information [169].

1
2
3
4
5
6
7
8
9
10
11
12
13
14
15
16
17
18
19
20
21
22
23
24
25
26
27
28
29
30
31
32
33
34
35
36
37
38
39
40
41
42
43
44
45
46
47
48
49
50
51
52
53
54
55
56
57
58
59
60
61
62
63
64
65

486 So far, feature extraction is an arduous and difficult task requiring the testing of
487 hundreds of feature extraction algorithms and a greater number of combinations
488 between them. This task demands expert skills in different subjects. The success in the
489 identification does not depend on the robustness of the classification methods, but on
490 the robustness of the data.

491

492 4. Machine Learning in plant image analysis

493

494 The amount of data generated in current and future phenomic setups with high
495 throughput imaging technologies has brought the use of Machine Learning (ML)
496 statistical approaches. Machine Learning is applied in many fields of research [170–
497 172]. As phenotyping can generate Terabytes of information, ML tools provide a good
498 framework for data analysis. A list of ML libraries can be found in Table 3. A major
499 advantage of ML is the possibility to explore large datasets to identify patterns, using
500 combinations of factors instead of performing independent analysis
501 [33].

502

503 Among the ML algorithms a predictive model of regression has been used to phenotype
504 Arabidopsis leaves, based on geometric features as training dataset [159]. Three
505 different algorithms were tested, k Nearest Neighbour (kNN), Support Vector Machine
506 (SVM) and Naïve Bayes to segment *Antirrhinum majus* leaves. Colour images have as a
507 characteristic vector intensity in the RGB and CIE $L^*a^*b^*$, while the NIR vector is
508 obtained with the wavelet transform. The best results were obtained with kNN for
509 colour images and SVM for NIR. This shows that segmentation has several components
510 as mentioned before including the wavelength of image acquisition [131].

511

512 As the specific wavelength used for image acquisition plays a key role in the type of
513 data obtained, hyperspectral cameras are becoming important tools, however, hyper
514 images can be in the order of Gbites of size, making ML a necessity. Examples of
515 coupling hyperspectral and thermal imaging with ML have allowed the early detection
516 of stress caused by *Alternaria* in Brassica [173]. The best image classification was
517 obtained doing a second derivative transformation of the hyperspectral images together
518 with a back propagation of neural networks allowing the identification of fungi on
519 leaves days after infection [173].

520

1 521 A current concept derived from ML is Deep Learning (DL) comprising a set of
2 algorithms aimed to model with a high level of abstraction. This allows the
3 development of complex concepts starting from simpler ones, thus getting closer to the
4 idea of Artificial Intelligence (AI) (www.deeplearningbook.org). Convolutional Neural
5 Networks (CNN), are an example of DL derived of Artificial Neural Networks (ANN).
6
7 These multi-layered networks are formed by a layer of neurons that work in a
8 convolutional way reducing the sampling process and end with a layer of perception
9 neurons for final classification [174]. Recently DL has been implemented using a CNN
10 to automatically classify and identify different plant parts [175], thus obtaining both
11 classification and localization that significantly improve the current methods. A CNN
12 has been used to detect plant pathogen attacks [176]. Although the training period is
13 computationally heavy, requiring several hours of CPU clusters, classification was
14 performed in less than one second [176]. Nevertheless, DL is a step forward in ML and
15 has great potential to allow the management and analysis of the data produced in
16 phenomic experiments.
17
18
19
20
21
22
23
24
25
26
27
28
29
30

536

31 Although direct testing maybe the best way to determine the superior algorithm in each
32 case, there is a number of examples that may guide initial approaches [33,177,178]. As
33 a general rule discriminating methods such as SVM, ANN, K-NN, give better results in
34 large datasets that are labelled [33]. Generative methods such as Naive Bayes, Gaussian
35 Mixture Models, Hide Markov Models, give better results with smaller datasets, both
36 labelled and unlabelled. The use of unsupervised algorithms i.e. k-means may help
37 identify unexpected characteristics on a dataset. As mentioned above, preprocessing
38 plays a fundamental role in increasing the ML output. A summary of the complete
39 pipeline of image analysis including sensors, preprocessing, segmentation procedures,
40 feature extractions and machine learning algorithms can be found in Table 4.
41
42
43
44
45
46
47
48
49
50

547

51 548 Conclusions and future prospects

52 549

53
54 550 The implementation of phenomic technologies is a welcome change towards
55 reproducibility and unbiased data acquisition in basic and applied research. A successful
56 approach requires integrating sensors, with wavelength and image acquisitions that will
57 allow the proper identification of the items under analysis. A lot of work has been made
58
59
60
61
62
63
64
65

1
2
3
4
5
6
7
8
9
10
11
12
13
14
15
16
17
18
19
20
21
22
23
24
25
26
27
28
29
30
31
32
33
34
35
36
37
38
39
40
41
42
43
44
45
46
47
48
49
50
51
52
53
54
55
56
57
58
59
60
61
62
63
64
65

554 in indoor-setups where reasonable conditions can be created to obtain high quality
555 images, amenable to further processing. The difficulty in outdoor setups increases as a
556 result of limitations in the actual image acquisition devices and the uncontrolled
557 conditions that directly affect image quality. The new technologies such as the high
558 definition LIDAR or the multi-hyperspectral cameras have a great potential to improve
559 in the near future, specially in outdoor environments.

560
561 The pre-processing and segmentation data are two aspects of data treatment and
562 acquisition that require careful design in order to avoid distortions and reproducibility
563 [138]. As images are machine-produced data, but image types and processing
564 procedures may be very different, the standardization of image capture, preprocessing
565 and segmentation may play an important role. Furthermore, a single procedure for
566 image analysis cannot be considered as a better choice and it is the researcher that needs
567 to assess the different algorithms to come with an optimized procedure for their specific
568 setup. It is a matter of time that databases with raw image will become part of the
569 standard in phenomics using images very much like NCBI or Uniprot play a key role in
570 genomic and proteomic projects. With the decrease in price of hyperspectral devices,
571 new experiments may be performed that produce even larger data sets, and these data
572 sets will have to go through Artificial Intelligence-based data analysis in order to give
573 the researchers results interpretable by humans. We guess that like in other omic
574 approaches, there will be a confluence to standard procedures that are not currently
575 common ground, making the current literature look intimidatingly diverse.
576 Nevertheless, most of the basic processes described here are shared by the different
577 experimental setups and data analysis pipes.

578

579 Abbreviations

580

581 **AI:** Artificial intelligence

582 **ANN:** Artificial neural networks

583 **CAI:** Cellulose Absorption Index

584 **CAR:** Chlorophyll absorption ratio

585 **CCD:** Charge coupled device

586 **Cig:** Coloration green

587 **Cir:** Coloration Index red

1
2
3
4
5
6
7
8
9
10
11
12
13
14
15
16
17
18
19
20
21
22
23
24
25
26
27
28
29
30
31
32
33
34
35
36
37
38
39
40
41
42
43
44
45
46
47
48
49
50
51
52
53
54
55
56
57
58
59
60
61
62
63
64
65

588 **CMOS:** Complementary metal oxide semiconductor
589 **CNN:** Convolutional neural networks
590 **CPU:** Central processing unit
591 **DL:** Deep learning
592 **DLAI:** Difference Leaf Area Index
593 **DSWI:** Disease water stress index
594 **DWT:** Daubechies wavelet transform
595 **EVI:** Enhanced vegetation index
596 **FAIR:** Findability, Accessibility, Interoperability, and Reusability
597 **GI:** Greenness Index
598 **GMM:** Gaussian mixture model
599 **GNDVI:** Green normalized difference vegetation index
600 **HOG:** Histograms of oriented gradients
601 **KNN:** K nearest neighbour
602 **LAI:** Leaf area index
603 **LCA:** Lignin-Cellulose Absorption Index
604 **LIDAR:** Light detection and ranging
605 **LWVI-1:** Normalized Difference Leaf water VI 1
606 **MCARI:** Modified Chlorophyll Absorption Ratio Index
607 **MCFI:** Multicolour fluorescence imaging
608 **ML:** Machine learning
609 **NDVI:** Normalized Difference Vegetation index
610 **NIR:** Near infrared
611 **NLI:** Nonlinear vegetation index
612 **NTDI:** Normalized Tillage Difference Index
613 **OSAVI:** Optimized Soil Adjusted Vegetation Index
614 **PCA:** Principal component analysis
615 **PWI:** Plant Water Index
616 **QTL:** Quantitative trait locus
617 **RGB:** Red, green, blue
618 **ROI:** Region of interest
619 **SIFT:** Scale invariant features transforms
620 **SURF:** Speeded-up robust features
621 **SVM:** Support vector machine

622 **TDI:** Time delay and integration
1
2 623 **ToF:** Time of flight
3
4 624
5
6 625 Competing interests
7 626
8
9 627 The authors declare they have no competing interests
10
11 628 Funding
12 629
13
14 630 This work was funded by grants FEDER BFU-2013-45148-R, Fundación Séneca
15 631 19398/PI/14 to MEC and FEDER ViSelTR (TIN2012-39279) to PJN
16
17 632
18
19 633 Availability of supporting data and material
20 634
21
22 635 Not applicable
23
24
25 636 Authors contributions
26 637
27
28 638 FPS, MEC and PJN defined the scope of the manuscript, FPS, MEC and PJN wrote and
29 639 corrected the manuscript, MEC and PJN wrote the grant applications.
30
31 640 Acknowledgments
32 641
33 642 We would like to thank Leanne Rebecca Miller for the edition of the manuscript and
34 643 Victoria Ruiz-Hernández and Julia Weiss for comments on the manuscript.
35
36 644
37
38 645 References
39 646
40
41 647 1. Tucker C. Red and photographic infrared linear combinations for monitoring
42 648 vegetation. *Remote Sens. Environ.* [Internet]. 1979 [cited 2016 Oct 11]; Available from:
43 649 <http://www.sciencedirect.com/science/article/pii/0034425779900130>
44
45 650 2. Myneni RB, Keeling CD, Tucker CJ, Asrar G, Nemani RR. Increased plant growth in the
46 651 northern high latitudes from 1981 to 1991. *Nature*. 1997;386:698–702.
47
48 652 3. DeFries R, Townshend J. NDVI-derived land cover classifications at a global scale. *Int.*
49 653 *J. Remote [Internet]*. 1994 [cited 2016 Oct 11]; Available from:
50
51 654 <http://www.tandfonline.com/doi/abs/10.1080/01431169408954345>
52
53 655 4. Pettorelli N, Vik J, Myserud A, Gaillard J. Using the satellite-derived NDVI to assess

1
2
3
4
5
6
7
8
9
10
11
12
13
14
15
16
17
18
19
20
21
22
23
24
25
26
27
28
29
30
31
32
33
34
35
36
37
38
39
40
41
42
43
44
45
46
47
48
49
50
51
52
53
54
55
56
57
58
59
60
61
62
63
64
65

656 ecological responses to environmental change. *Trends Ecol.* [Internet]. 2005 [cited
657 2016 Oct 11]; Available from:
658 <http://www.sciencedirect.com/science/article/pii/S016953470500162X>
659 5. Mkhabela MS, Bullock P, Raj S, Wang S, Yang Y. Crop yield forecasting on the
660 Canadian Prairies using MODIS NDVI data. *Agric. For. Meteorol.* 2011;151:385–93.
661 6. GROTEN SME. NDVI—crop monitoring and early yield assessment of Burkina Faso.
662 *Int. J. Remote Sens.* [Internet]. Taylor & Francis Group ; 1993 [cited 2016 Dec
663 6];14:1495–515. Available from:
664 <http://www.tandfonline.com/doi/abs/10.1080/01431169308953983>
665 7. Jones HG, Stoll M, Santos T, de Sousa C, Chaves MM, Grant OM. Use of infrared
666 thermography for monitoring stomatal closure in the field: application to grapevine. *J.*
667 *Exp. Bot.* [Internet]. Oxford University Press; 2002 [cited 2016 Dec 6];53:2249–60.
668 Available from: <http://www.ncbi.nlm.nih.gov/pubmed/12379792>
669 8. Chaerle L, Van der Straeten D. Seeing is believing: imaging techniques to monitor
670 plant health. *Biochim. Biophys. Acta-Gene Struct. Expr.* 2001;1519:153–66.
671 9. Sirault XRR, James RA, Furbank RT, Bernstein L, Hayward H, Flowers T, et al. A new
672 screening method for osmotic component of salinity tolerance in cereals using infrared
673 thermography. *Funct. Plant Biol.* [Internet]. CSIRO PUBLISHING; 2009 [cited 2016 Dec
674 6];36:970. Available from: <http://www.publish.csiro.au/?paper=FP09182>
675 10. Lobet G, Pagès L, Draye X. A Novel Image Analysis Toolbox Enabling Quantitative
676 Analysis of Root System Architecture. *Plant Physiol.* [Internet]. 2011;157:29–39.
677 Available from: <http://www.ncbi.nlm.nih.gov/pubmed/21771915>
678 11. Galkovskyi T, Mileyko Y, Bucksch A, Moore B, Symonova O, Price CA, et al. GiA
679 Roots: software for the high throughput analysis of plant root system architecture.
680 *BMC Plant Biol.* [Internet]. BioMed Central; 2012 [cited 2016 Sep 10];12:116. Available
681 from: <http://bmcpantbiol.biomedcentral.com/articles/10.1186/1471-2229-12-116>
682 12. French A, Ubeda-Tomas S, Holman TJ, Bennett MJ, Pridmore T. High-Throughput
683 Quantification of Root Growth Using a Novel Image-Analysis Tool. *Plant Physiol.*
684 [Internet]. American Society of Plant Biologists; 2009 [cited 2016 Sep 20];150:1784–95.
685 Available from:
686 <http://www.pubmedcentral.nih.gov/articlerender.fcgi?artid=2719150&tool=pmcentre>
687 [z&rendertype=abstract](http://www.pubmedcentral.nih.gov/articlerender.fcgi?artid=2719150&tool=pmcentre)

1
2
3
4
5
6
7
8
9
10
11
12
13
14
15
16
17
18
19
20
21
22
23
24
25
26
27
28
29
30
31
32
33
34
35
36
37
38
39
40
41
42
43
44
45
46
47
48
49
50
51
52
53
54
55
56
57
58
59
60
61
62
63
64
65

688 13. Golzarian MR, Frick RA, Rajendran K, Berger B, Roy S, Tester M, et al. Accurate
689 inference of shoot biomass from high-throughput images of cereal plants. *Plant*
690 *Methods* [Internet]. BioMed Central; 2011 [cited 2016 Sep 10];7:2. Available from:
691 <http://plantmethods.biomedcentral.com/articles/10.1186/1746-4811-7-2>

692 14. Fabre J, Dauzat M, Negre V, Wuyts N, Tireau A, Gennari E, et al. PHENOPSIS DB: an
693 Information System for Arabidopsis thaliana phenotypic data in an environmental
694 context. *BMC Plant Biol.* 2011;11.

695 15. Araus JL, Cairns JE. Field high-throughput phenotyping: The new crop breeding
696 frontier. *Trends Plant Sci.* 2014;19:52–61.

697 16. Furbank RT. Plant phenomics: from gene to form and function. *Funct. Plant Biol.*
698 [Internet]. 2009 [cited 2016 Aug 31];36:V–Vi. Available from:
699 [http://citeseerx.ist.psu.edu/viewdoc/download?doi=10.1.1.547.5673&rep=rep1&type](http://citeseerx.ist.psu.edu/viewdoc/download?doi=10.1.1.547.5673&rep=rep1&type=pdf)
700 [=pdf](#)

701 17. Poorter H, Fiorani F, Pieruschka R, Putten WH Van Der, Kleyer M, Schurr U. Tansley
702 review Pampered inside , pestered outside ? Differences and similarities between
703 plants growing in controlled conditions and in the field. *New Phytol.* 2016;838–55.

704 18. Yang W, Duan L, Chen G, Xiong L, Liu Q. Plant phenomics and high-throughput
705 phenotyping: Accelerating rice functional genomics using multidisciplinary
706 technologies. *Curr. Opin. Plant Biol.* [Internet]. Elsevier Ltd; 2013;16:180–7. Available
707 from: <http://dx.doi.org/10.1016/j.pbi.2013.03.005>

708 19. White J, Andrade-Sanchez P, Gore M. Field-based phenomics for plant genetics
709 research. *F. Crop.* [Internet]. 2012 [cited 2016 Aug 31]; Available from:
710 <http://www.sciencedirect.com/science/article/pii/S037842901200130X>

711 20. Fahlgren N, Gehan MA, Baxter I. Lights, camera, action: High-throughput plant
712 phenotyping is ready for a close-up. *Curr. Opin. Plant Biol.* 2015. p. 93–9.

713 21. Furbank RT, Tester M. Phenomics - technologies to relieve the phenotyping
714 bottleneck. *Trends Plant Sci.* 2011;16:635–44.

715 22. Granier C, Vile D. Phenotyping and beyond: Modelling the relationships between
716 traits. *Curr. Opin. Plant Biol.* [Internet]. Elsevier Ltd; 2014;18:96–102. Available from:
717 <http://dx.doi.org/10.1016/j.pbi.2014.02.009>

718 23. White J, Andrade-Sanchez P, Gore M. Field-based phenomics for plant genetics
719 research. *F. Crop.* 2012;

1 720 24. Furbank RT, Tester M. Phenomics - technologies to relieve the phenotyping
2 721 bottleneck. *Trends Plant Sci.* 2011;16:635–44.

3 722 25. Simko I, Jimenez-Berni JA, Sirault XRR. Phenomic approaches and tools for
4 723 phytopathologists. *Phytopathology* [Internet]. 2016;PHYTO-02-16-0082-RVW. Available
5 724 from: <http://apsjournals.apsnet.org/doi/10.1094/PHYTO-02-16-0082-RVW>

6 725 26. da Silva Marques J. Monitoring Photosynthesis by In Vivo Chlorophyll
7 726 Fluorescence : Application to High-Throughput Plant Phenotyping. *Appl. Photosynth. -*
8 727 *New Prog.* 2016;Intech:3–22.

9 728 27. Gonzalez RC, Woods RE. *Digital image processing.* Prentice Hall Press ; 2002.

10 729 28. Russ J, Woods R. *The image processing handbook.* 1995 [cited 2017 Apr 25];
11 730 Available from:
12 731 [http://journals.lww.com/jcat/Citation/1995/11000/The_Image_Processing_Handbook,](http://journals.lww.com/jcat/Citation/1995/11000/The_Image_Processing_Handbook,_)
13 732 [_2nd_Ed.26.aspx](http://journals.lww.com/jcat/Citation/1995/11000/The_Image_Processing_Handbook,_)

14 733 29. Jain A. *Fundamentals of digital image processing.* 1989 [cited 2017 Apr 25];
15 734 Available from: <http://dl.acm.org/citation.cfm?id=59921>

16 735 30. Sonka M, Hlavac V, Boyle R. *Image processing, analysis, and machine vision*
17 736 [Internet]. 4th ed. CL Engineering; 2014 [cited 2017 Apr 24]. Available from:
18 737 <https://books.google.es/books?hl=en&lr=&id=QePKAgAAQBAJ&oi=fnd&pg=PR11&dq=>
19 738 [image+analysis+a+review&ots=95qB21F9B-&sig=kSGTMS9GfxkddVJUHNxnBzU2VL8](https://books.google.es/books?hl=en&lr=&id=QePKAgAAQBAJ&oi=fnd&pg=PR11&dq=)

20 739 31. Soille P. *Morphological image analysis: principles and applications* [Internet].
21 740 Springer; 2013 [cited 2017 Apr 24]. Available from:
22 741 <https://books.google.es/books?hl=en&lr=&id=ZFzxCAAQBAJ&oi=fnd&pg=PA1&dq=i>
23 742 [mage+analysis+a+review&ots=-oc-0SEZ6g&sig=wLoRbdNSusr-5UtgD_RvtMHVqjQ](https://books.google.es/books?hl=en&lr=&id=ZFzxCAAQBAJ&oi=fnd&pg=PA1&dq=i)

24 743 32. Li L, Zhang Q, Huang D. A Review of Imaging Techniques for Plant Phenotyping.
25 744 *Sensors.* 2014;14:20078–111.

26 745 33. Singh A, Ganapathysubramanian B, Singh AK, Sarkar S. Machine Learning for High-
27 746 Throughput Stress Phenotyping in Plants. *Trends Plant Sci.* 2016. p. 110–24.

28 747 34. Fiorani F, Schurr U. Future Scenarios for Plant Phenotyping. *Annu. Rev. Plant Biol*
29 748 [Internet]. 2013 [cited 2016 Sep 21];64:267–91. Available from:
30 749 <http://www.ncbi.nlm.nih.gov/pubmed/23451789>

31 750 35. Lepage G, Bogaerts J, Meynants G. Time-delay-integration architectures in CMOS
32 751 image sensors. *IEEE Trans. Electron Devices* [Internet]. 2009 [cited 2017 Apr

752 26];56:2524–33. Available from:
1
2 753 <http://s3.amazonaws.com/academia.edu.documents/34420865/05272462.pdf?AWSAccessKeyId=AKIAIWOWYYGZ2Y53UL3A&Expires=1493227777&Signature=%2BCCwsvCdYXhWhL83LxFrED1f9pY%3D&response-content-disposition=inline%3Bfilename%3D05272462.pdf>
3
4 754
5 755
6 756
7
8
9 757 36. Yu C, Nie K, Xu J, Gao J. A Low Power Digital Accumulation Technique for Digital-
10
11 758 Domain CMOS TDI Image Sensor. *Sensors* [Internet]. Multidisciplinary Digital
12
13 759 Publishing Institute; 2016 [cited 2017 Apr 24];16:1572. Available from:
14
15 760 <http://www.mdpi.com/1424-8220/16/10/1572>
16
17 761 37. Teledyne Dalsa. No Title. <https://www.teledynedalsa.com/corp/>.
18
19 762 38. IMEC. Imec launches TDI, multispectral and hyperspectral sensors [Internet]. [cited
20
21 763 2017 Apr 24]. Available from: <http://optics.org/news/8/2/8>
22
23 764 39. Van Der Heijden G, Song Y, Horgan G, Polder G, Dieleman A, Bink M, et al. SPICY:
24
25 765 Towards automated phenotyping of large pepper plants in the greenhouse. *Funct.*
26
27 766 *Plant Biol.* CSIRO PUBLISHING; 2012;39:870–7.
28
29 767 40. Navarro PJ, Fernández C, Weiss J, Egea-Cortines M. Development of a configurable
30
31 768 growth chamber with a computer vision system to study circadian rhythm in plants.
32
33 769 *Sensors* (Basel). [Internet]. 2012 [cited 2016 Sep 20];12:15356–75. Available from:
34
35 770 <http://www.ncbi.nlm.nih.gov/pubmed/23202214>
36
37 771 41. Subramanian R, Spalding EP, Ferrier NJ. A high throughput robot system for
38
39 772 machine vision based plant phenotype studies. *Mach. Vis. Appl.* [Internet].
40
41 773 2013;24:619–36. Available from: <http://link.springer.com/10.1007/s00138-012-0434-4>
42
43 774 42. Zhang X, Huang C, Wu D, Qiao F, Li W, Duan L, et al. High-throughput phenotyping
44
45 775 and QTL mapping reveals the genetic architecture of maize plant growth. *Plant Physiol.*
46
47 776 [Internet]. 2017;pp.01516.2016. Available from:
48
49 777 <http://www.plantphysiol.org/lookup/doi/10.1104/pp.16.01516>
50
51 778 43. Virlet N, Sabermanesh K, Sadeghi-Tehran P, Hawkesford MJ. Field Scanalyzer: An
52
53 779 automated robotic field phenotyping platform for detailed crop monitoring. *Funct.*
54
55 780 *Plant Biol.* [Internet]. 2017 [cited 2017 May 11];44:143. Available from:
56
57 781 <http://www.publish.csiro.au/?paper=FP16163>
58
59 782 44. Deery D, Jimenez-Berni J, Jones H, Sirault X, Furbank R. Proximal Remote Sensing
60
61 783 Buggies and Potential Applications for Field-Based Phenotyping. *Agronomy* [Internet].
62
63
64
65

1
2
3
4
5
6
7
8
9
10
11
12
13
14
15
16
17
18
19
20
21
22
23
24
25
26
27
28
29
30
31
32
33
34
35
36
37
38
39
40
41
42
43
44
45
46
47
48
49
50
51
52
53
54
55
56
57
58
59
60
61
62
63
64
65

784 Multidisciplinary Digital Publishing Institute; 2014 [cited 2017 May 23];4:349–79.
785 Available from: <http://www.mdpi.com/2073-4395/4/3/349/>

786 45. Comar A, Burger P, de Solan B, Baret F, Daumard F, Hanocq J-F, et al. A semi-
787 automatic system for high throughput phenotyping wheat cultivars in-field conditions:
788 description and first results. *Funct. Plant Biol.* CSIRO PUBLISHING; 2012;39:914.

789 46. Brown MZ, Burschka D, Hager GD. Advances in computational stereo. *IEEE Trans.*
790 *Pattern Anal. Mach. Intell.* [Internet]. 2003 [cited 2017 Apr 26];25:993–1008. Available
791 from: <http://ieeexplore.ieee.org/document/1217603/>

792 47. Biskup B, Scharr H, Schurr U, Rascher U. A stereo imaging system for measuring
793 structural parameters of plant canopies. *Plant, Cell Environ.* [Internet]. Blackwell
794 Publishing Ltd; 2007 [cited 2016 Sep 20];30:1299–308. Available from:
795 <http://doi.wiley.com/10.1111/j.1365-3040.2007.01702.x>

796 48. Nguyen TT, Slaughter DC, Max N, Maloof JN, Sinha N. Structured light-based 3D
797 reconstruction system for plants. *Sensors (Switzerland)* [Internet]. Multidisciplinary
798 Digital Publishing Institute; 2015 [cited 2016 Sep 21];15:18587–612. Available from:
799 <http://www.mdpi.com/1424-8220/15/8/18587/>

800 49. Klodt M, Herzog K, Töpfer R, Cremers D, Töpfer R, Hausmann L, et al. Field
801 phenotyping of grapevine growth using dense stereo reconstruction. *BMC*
802 *Bioinformatics* [Internet]. BioMed Central; 2015 [cited 2016 Oct 7];16:143. Available
803 from: <http://www.biomedcentral.com/1471-2105/16/143>

804 50. Rose J, Kicherer A, Wieland M, Klingbeil L, Töpfer R, Kuhlmann H. Towards
805 Automated Large-Scale 3D Phenotyping of Vineyards under Field Conditions. *Sensors*
806 [Internet]. Multidisciplinary Digital Publishing Institute; 2016 [cited 2017 May
807 11];16:2136. Available from: <http://www.mdpi.com/1424-8220/16/12/2136>

808 51. Xiong X, Yu L, Yang W, Liu M, Jiang N, Wu D, et al. A high-throughput stereo-
809 imaging system for quantifying rape leaf traits during the seedling stage. *Plant*
810 *Methods* [Internet]. BioMed Central; 2017 [cited 2017 Feb 8];13:7. Available from:
811 <http://plantmethods.biomedcentral.com/articles/10.1186/s13007-017-0157-7>

812 52. Paproki A, Sirault XRR, Berry S, Furbank RT, Fripp J. A novel mesh processing based
813 technique for 3D plant analysis. *BMC Plant Biol.* [Internet]. 2012;12:63. Available from:
814 <http://www.biomedcentral.com/1471-2229/12/63>

815 53. Nguyen TT, Slaughter DC, Maloof JN, Sinha N. Plant phenotyping using multi-view

1
2
3
4
5
6
7
8
9
10
11
12
13
14
15
16
17
18
19
20
21
22
23
24
25
26
27
28
29
30
31
32
33
34
35
36
37
38
39
40
41
42
43
44
45
46
47
48
49
50
51
52
53
54
55
56
57
58
59
60
61
62
63
64
65

816 stereo vision with structured lights. In: Valasek J, Thomasson JA, editors. International
817 Society for Optics and Photonics; 2016 [cited 2017 May 19]. p. 986608. Available from:
818 <http://proceedings.spiedigitallibrary.org/proceeding.aspx?doi=10.1117/12.2229513>
819 54. Rose JC, Paulus S, Kuhlmann H. Accuracy analysis of a multi-view stereo approach
820 for phenotyping of tomato plants at the organ level. *Sensors (Basel)*. [Internet].
821 Multidisciplinary Digital Publishing Institute (MDPI); 2015 [cited 2017 May
822 19];15:9651–65. Available from: <http://www.ncbi.nlm.nih.gov/pubmed/25919368>
823 55. Schwartz S. An overview of 3D plant phenotyping methods [Internet]. *Phenospex*.
824 *Smart Plant Analysis*. 2015 [cited 2017 Jun 19]. Available from:
825 <https://phenospex.com/blog/an-overview-of-3d-plant-phenotyping-methods/#ref>
826 56. Lee K-S, Cohen WB, Kennedy RE, Maiersperger TK, Gower ST. Hyperspectral versus
827 multispectral data for estimating leaf area index in four different biomes. *Remote*
828 *Sens. Environ.* [Internet]. 2004 [cited 2017 Apr 27];91:508–20. Available from:
829 <http://www.sciencedirect.com/science/article/pii/S0034425704001282>
830 57. Dozier J, Painter TH. MULTISPECTRAL AND HYPERSPECTRAL REMOTE SENSING OF
831 ALPINE SNOW PROPERTIES. *Annu. Rev. Earth Planet. Sci.* [Internet]. *Annual Reviews*;
832 2004 [cited 2017 Apr 27];32:465–94. Available from:
833 <http://www.annualreviews.org/doi/10.1146/annurev.earth.32.101802.120404>
834 58. Adam E, Mutanga O, Rugege D. Multispectral and hyperspectral remote sensing for
835 identification and mapping of wetland vegetation: a review. *Wetl. Ecol. Manag.*
836 [Internet]. Springer Netherlands; 2010 [cited 2017 Apr 27];18:281–96. Available from:
837 <http://link.springer.com/10.1007/s11273-009-9169-z>
838 59. Qin J, Chao K, Kim MS, Lu R, Burks TF. Hyperspectral and multispectral imaging for
839 evaluating food safety and quality. *J. Food Eng.* [Internet]. 2013 [cited 2017 Apr
840 27];118:157–71. Available from:
841 <http://www.sciencedirect.com/science/article/pii/S0260877413001659>
842 60. van der Meer FD, van der Werff HMA, van Ruitenbeek FJA, Hecker CA, Bakker WH,
843 Noomen MF, et al. Multi- and hyperspectral geologic remote sensing: A review. *Int. J.*
844 *Appl. Earth Obs. Geoinf.* [Internet]. 2012 [cited 2017 Apr 27];14:112–28. Available
845 from: <http://www.sciencedirect.com/science/article/pii/S0303243411001103>
846 61. P. M. Mehl PM, K. Chao K, M. Kim M, Y. R. Chen YR. DETECTION OF DEFECTS ON
847 SELECTED APPLE CULTIVARS USING HYPERSPECTRAL AND MULTISPECTRAL IMAGE

1
2
3
4
5
6
7
8
9
10
11
12
13
14
15
16
17
18
19
20
21
22
23
24
25
26
27
28
29
30
31
32
33
34
35
36
37
38
39
40
41
42
43
44
45
46
47
48
49
50
51
52
53
54
55
56
57
58
59
60
61
62
63
64
65

848 ANALYSIS. Appl. Eng. Agric. [Internet]. American Society of Agricultural and Biological
849 Engineers; 2002 [cited 2017 Apr 27];18:219. Available from:
850 <http://elibrary.asabe.org/abstract.asp??JID=3&AID=7790&CID=aeaj2002&v=18&i=2&T>
851 =1
852 62. Ferrato L-J. COMPARING HYPERSPECTRAL AND MULTISPECTRAL IMAGERY FOR
853 LAND CLASSIFICATION OF THE LOWER DON RIVER, TORONTO. [cited 2017 Apr 27];
854 Available from:
855 <http://www.geography.ryerson.ca/wayne/MSA/LisaJenFerratoMRP2012.pdf>
856 63. Cubert. S 137 - ButterfIEYE NIR - Cubert-GmbH [Internet]. [cited 2017 Jun 4].
857 Available from: <http://cubert-gmbh.com/product/s-137-butterfleye-nir/>
858 64. Kise M, Park B, Heitschmidt GW, Lawrence KC, Windham WR. Multispectral
859 imaging system with interchangeable filter design. Comput. Electron. Agric.
860 2010;72:61–8.
861 65. Li P, Lee S-H, Hsu H-Y, Park J-S. Nonlinear Fusion of Multispectral Citrus Fruit Image
862 Data with Information Contents. Sensors [Internet]. Multidisciplinary Digital Publishing
863 Institute; 2017 [cited 2017 Jan 23];17:142. Available from:
864 <http://www.mdpi.com/1424-8220/17/1/142>
865 66. Wahabzada M, Mahlein A-K, Bauckhage C, Steiner U, Oerke E-C, Kersting K. Plant
866 Phenotyping using Probabilistic Topic Models: Uncovering the Hyperspectral Language
867 of Plants. Sci. Rep. [Internet]. Nature Publishing Group; 2016 [cited 2017 Jan
868 24];6:22482. Available from: <http://www.ncbi.nlm.nih.gov/pubmed/26957018>
869 67. Kuska M, Wahabzada M, Leucker M, Dehne H-W, Kersting K, Oerke E-C, et al.
870 Hyperspectral phenotyping on the microscopic scale: towards automated
871 characterization of plant-pathogen interactions. Plant Methods [Internet]. 2015 [cited
872 2017 May 11];11:28. Available from: <http://www.plantmethods.com/content/11/1/28>
873 68. Klose R, Penlington J. Usability study of 3D time-of-flight cameras for automatic
874 plant phenotyping. Bornimer [Internet]. 2009 [cited 2017 May 2]; Available from:
875 [https://www.hs-](https://www.hs-osnabrueck.de/fileadmin/HSOS/Homepages/COALA/Veroeffentlichungen/2009-CBA-3DToF.pdf)
876 [osnabrueck.de/fileadmin/HSOS/Homepages/COALA/Veroeffentlichungen/2009-CBA-](https://www.hs-osnabrueck.de/fileadmin/HSOS/Homepages/COALA/Veroeffentlichungen/2009-CBA-3DToF.pdf)
877 [3DToF.pdf](https://www.hs-osnabrueck.de/fileadmin/HSOS/Homepages/COALA/Veroeffentlichungen/2009-CBA-3DToF.pdf)
878 69. Song Y, Glasbey CA, van der Heijden GWAM, Polder G, Dieleman JA. Combining
879 Stereo and Time-of-Flight Images with Application to Automatic Plant Phenotyping.

1
2
3
4
5
6
7
8
9
10
11
12
13
14
15
16
17
18
19
20
21
22
23
24
25
26
27
28
29
30
31
32
33
34
35
36
37
38
39
40
41
42
43
44
45
46
47
48
49
50
51
52
53
54
55
56
57
58
59
60
61
62
63
64
65

880 Springer Berlin Heidelberg; 2011. p. 467–78.

881 70. Alenyà G, Dellen B, Torras C. 3D modelling of leaves from color and ToF data for
882 robotized plant measuring. Robot. Autom. (ICRA), [Internet]. 2011 [cited 2017 May 2];
883 Available from: <http://ieeexplore.ieee.org/abstract/document/5980092/>

884 71. McCormick RF, Truong SK, Mullet JE. 3D Sorghum Reconstructions from Depth
885 Images Identify QTL Regulating Shoot Architecture. Plant Physiol. [Internet]. American
886 Society of Plant Biologists; 2016 [cited 2017 May 2];172:823–34. Available from:
887 <http://www.ncbi.nlm.nih.gov/pubmed/27528244>

888 72. Paulus S, Behmann J, Mahlein A, Plümer L. Low-cost 3D systems: suitable tools for
889 plant phenotyping. Sensors [Internet]. 2014 [cited 2017 May 2]; Available from:
890 <http://www.mdpi.com/1424-8220/14/2/3001/htm>

891 73. Microsoft. Kinect for Windows Sensor Components and Specifications [Internet].
892 2010. [cited 2017 May 7]. Available from: [https://msdn.microsoft.com/en-](https://msdn.microsoft.com/en-us/library/jj131033.aspx)
893 [us/library/jj131033.aspx](https://msdn.microsoft.com/en-us/library/jj131033.aspx)

894 74. Azzari G, Goulden M, Rusu R. Rapid Characterization of Vegetation Structure with a
895 Microsoft Kinect Sensor. Sensors [Internet]. Multidisciplinary Digital Publishing
896 Institute; 2013 [cited 2017 May 7];13:2384–98. Available from:
897 <http://www.mdpi.com/1424-8220/13/2/2384/>

898 75. Chéné Y, Rousseau D, Lucidarme P, Bertheloot J, Caffier V, Morel P, et al. On the
899 use of depth camera for 3D phenotyping of entire plants. Comput. Electron. Agric.
900 2012;82:122–7.

901 76. Wang G, Weng Q. Remote sensing of natural resources. [cited 2017 May 9]. p. 532.
902 Available from:
903 [https://books.google.es/books?id=wIDNBQAAQBAJ&pg=PA9&dq=Light+Detection+an](https://books.google.es/books?id=wIDNBQAAQBAJ&pg=PA9&dq=Light+Detection+and+Ranging+(LIDAR)+1970s&hl=es&sa=X&ved=0ahUKEwi0mbSksePTAhVJDxoKHaKxC6UQ6AEIJjAA#v=onepage&q=Light+Detection+and+Ranging+(LIDAR)+1970s&f=false)
904 [d+Ranging+\(LIDAR\)+1970s&hl=es&sa=X&ved=0ahUKEwi0mbSksePTAhVJDxoKHaKxC6U](https://books.google.es/books?id=wIDNBQAAQBAJ&pg=PA9&dq=Light+Detection+and+Ranging+(LIDAR)+1970s&hl=es&sa=X&ved=0ahUKEwi0mbSksePTAhVJDxoKHaKxC6UQ6AEIJjAA#v=onepage&q=Light+Detection+and+Ranging+(LIDAR)+1970s&f=false)
905 [Q6AEIJjAA#v=onepage&q=Light Detection and Ranging \(LIDAR\) 1970s&f=false](https://books.google.es/books?id=wIDNBQAAQBAJ&pg=PA9&dq=Light+Detection+and+Ranging+(LIDAR)+1970s&hl=es&sa=X&ved=0ahUKEwi0mbSksePTAhVJDxoKHaKxC6UQ6AEIJjAA#v=onepage&q=Light+Detection+and+Ranging+(LIDAR)+1970s&f=false)

906 77. Lin Y. LiDAR: An important tool for next-generation phenotyping technology of high
907 potential for plant phenomics? Comput. Electron. Agric. Elsevier B.V.; 2015;119:61–73.

908 78. Vázquez-Arellano M, Griepentrog HW, Reiser D, Paraforos DS. 3-D Imaging Systems
909 for Agricultural Applications-A Review. Sensors (Basel). [Internet]. Multidisciplinary
910 Digital Publishing Institute (MDPI); 2016 [cited 2017 May 2];16. Available from:
911 <http://www.ncbi.nlm.nih.gov/pubmed/27136560>

1
2
3
4
5
6
7
8
9
10
11
12
13
14
15
16
17
18
19
20
21
22
23
24
25
26
27
28
29
30
31
32
33
34
35
36
37
38
39
40
41
42
43
44
45
46
47
48
49
50
51
52
53
54
55
56
57
58
59
60
61
62
63
64
65

912 79. Chen JM, Cihlar J. Retrieving leaf area index of boreal conifer forests using Landsat
913 TM images. *Remote Sens. Environ.* [Internet]. 1996 [cited 2016 Sep 26];55:155–62.
914 Available from: <http://linkinghub.elsevier.com/retrieve/pii/0034425795001956>
915 80. Gwenzi D, Helmer E, Zhu X, Lefsky M, Marcano-Vega H. Predictions of Tropical
916 Forest Biomass and Biomass Growth Based on Stand Height or Canopy Area Are
917 Improved by Landsat-Scale Phenology across Puerto Rico and the U.S. Virgin Islands.
918 *Remote Sens.* [Internet]. Multidisciplinary Digital Publishing Institute; 2017 [cited 2017
919 May 9];9:123. Available from: <http://www.mdpi.com/2072-4292/9/2/123>
920 81. Kellndorfer JM, Walker WS, LaPoint E, Kirsch K, Bishop J, Fiske G. Statistical fusion
921 of lidar, InSAR, and optical remote sensing data for forest stand height
922 characterization: A regional-scale method based on LVIS, SRTM, Landsat ETM+, and
923 ancillary data sets. *J. Geophys. Res. Biogeosciences* [Internet]. 2010 [cited 2017 May
924 9];115:n/a-n/a. Available from: <http://doi.wiley.com/10.1029/2009JG000997>
925 82. Badreldin N, Sanchez-Azofeifa A. Estimating Forest Biomass Dynamics by
926 Integrating Multi-Temporal Landsat Satellite Images with Ground and Airborne LiDAR
927 Data in the Coal Valley Mine, Alberta, Canada. *Remote Sens.* [Internet].
928 Multidisciplinary Digital Publishing Institute; 2015 [cited 2017 May 9];7:2832–49.
929 Available from: <http://www.mdpi.com/2072-4292/7/3/2832/>
930 83. Andújar D, Rueda-Ayala V, Moreno H, Rosell-Polo JR, Escolà A, Valero C, et al.
931 Discriminating crop, weeds and soil surface with a terrestrial LIDAR sensor. *Sensors*
932 (Switzerland) [Internet]. Multidisciplinary Digital Publishing Institute; 2013 [cited 2017
933 May 8];13:14662–75. Available from: <http://www.mdpi.com/1424-8220/13/11/14662/>
934 84. Sun S, Li C, Paterson A. In-Field High-Throughput Phenotyping of Cotton Plant
935 Height Using LiDAR. *Remote Sens.* [Internet]. Multidisciplinary Digital Publishing
936 Institute; 2017 [cited 2017 May 8];9:377. Available from: <http://www.mdpi.com/2072-4292/9/4/377>
937 85. Hosoi F, Nakabayashi K, Omasa K. 3-D modeling of tomato canopies using a high-
938 resolution portable scanning lidar for extracting structural information. *Sensors*
939 (Basel). [Internet]. Multidisciplinary Digital Publishing Institute (MDPI); 2011 [cited
940 2017 May 7];11:2166–74. Available from:
941 <http://www.ncbi.nlm.nih.gov/pubmed/22319403>
942 86. Chaudhury A, Ward C, Talasaz A, Ivanov AG, Norman PAH, Grodzinski B, et al.

1
2
3
4
5
6
7
8
9
10
11
12
13
14
15
16
17
18
19
20
21
22
23
24
25
26
27
28
29
30
31
32
33
34
35
36
37
38
39
40
41
42
43
44
45
46
47
48
49
50
51
52
53
54
55
56
57
58
59
60
61
62
63
64
65

944 Computer Vision Based Autonomous Robotic System for 3D Plant Growth
945 Measurement. 12th Conf. Comput. Robot Vis. 2015;290–6.
946 87. Kjaer KH, Ottosen C-O. 3D Laser Triangulation for Plant Phenotyping in Challenging
947 Environments. *Sensors* (Basel). [Internet]. Multidisciplinary Digital Publishing Institute
948 (MDPI); 2015 [cited 2017 Jan 18];15:13533–47. Available from:
949 <http://www.ncbi.nlm.nih.gov/pubmed/26066990>
950 88. Lin Y. LiDAR: An important tool for next-generation phenotyping technology of high
951 potential for plant phenomics? *Comput. Electron. Agric.* [Internet]. 2015 [cited 2017
952 May 8];119:61–73. Available from:
953 <http://www.sciencedirect.com/science/article/pii/S0168169915003245>
954 89. Wallace A, Nichol C, Woodhouse I. Recovery of Forest Canopy Parameters by
955 Inversion of Multispectral LiDAR Data. *Remote Sens.* [Internet]. Molecular Diversity
956 Preservation International; 2012 [cited 2017 May 19];4:509–31. Available from:
957 <http://www.mdpi.com/2072-4292/4/2/509/>
958 90. Morsy S, Shaker A, El-Rabbany A. Multispectral LiDAR Data for Land Cover
959 Classification of Urban Areas. *Sensors* [Internet]. 2017 [cited 2017 May 19];17:958.
960 Available from: <http://www.ncbi.nlm.nih.gov/pubmed/28445432>
961 91. Wallace AM, McCarthy A, Nichol CJ, Ximing Ren, Morak S, Martinez-Ramirez D, et
962 al. Design and Evaluation of Multispectral LiDAR for the Recovery of Arboreal
963 Parameters. *IEEE Trans. Geosci. Remote Sens.* [Internet]. 2014 [cited 2017 May
964 19];52:4942–54. Available from: <http://ieeexplore.ieee.org/document/6672004/>
965 92. Navarro P, Fernández C, Borraz R, Alonso D. A Machine Learning Approach to
966 Pedestrian Detection for Autonomous Vehicles Using High-Definition 3D Range Data.
967 *Sensors*. Multidisciplinary Digital Publishing Institute; 2016;17:18.
968 93. Padhi J, Misra RK, Payero JO. Estimation of soil water deficit in an irrigated cotton
969 field with infrared thermography. *F. Crop. Res.* [Internet]. 2012 [cited 2017 May
970 12];126:45–55. Available from:
971 <http://linkinghub.elsevier.com/retrieve/pii/S0378429011003303>
972 94. Guilioni L, Jones HG, Leinonen I, Lhomme JP. On the relationships between
973 stomatal resistance and leaf temperatures in thermography. *Agric. For. Meteorol.*
974 [Internet]. 2008 [cited 2017 May 12];148:1908–12. Available from:
975 <http://linkinghub.elsevier.com/retrieve/pii/S0168192308002074>

1 976 95. Kranner I, Kastberger G, Hartbauer M, Pritchard HW. Noninvasive diagnosis of seed
2 977 viability using infrared thermography. Proc. Natl. Acad. Sci. [Internet]. 2010 [cited 2017
3
4 978 May 12];107:3912–7. Available from:
5
6 979 <http://www.pnas.org/cgi/doi/10.1073/pnas.0914197107>
7
8 980 96. Jones HG. Use of infrared thermography for monitoring stomatal closure in the
9
10 981 field: application to grapevine. J. Exp. Bot. [Internet]. 2002 [cited 2017 May
11
12 982 12];53:2249–60. Available from: [https://academic.oup.com/jxb/article-](https://academic.oup.com/jxb/article-lookup/doi/10.1093/jxb/erf083)
13
14 983 [lookup/doi/10.1093/jxb/erf083](https://academic.oup.com/jxb/article-lookup/doi/10.1093/jxb/erf083)
15
16 984 97. Fiorani F, Rascher U, Jahnke S, Schurr U. Imaging plants dynamics in heterogenic
17
18 985 environments. Curr. Opin. Biotechnol. [Internet]. 2012 [cited 2017 May 12];23:227–35.
19
20 986 Available from:
21
22 987 <http://www.sciencedirect.com/science/article/pii/S0958166911007531>
23
24 988 98. Mallona I, Egea-Cortines M, Weiss J. Conserved and divergent rhythms of CAM-
25
26 989 related and core clock gene expression in the cactus *Opuntia ficus-indica*. Plant Physiol.
27
28 990 2011;156:1978–89.
29
30 991 99. Somers DE, Webb a a, Pearson M, Kay S a. The short-period mutant, *toc1-1*, alters
31
32 992 circadian clock regulation of multiple outputs throughout development in *Arabidopsis*
33
34 993 *thaliana*. Development [Internet]. 1998;125:485–94. Available from:
35
36 994 <http://www.ncbi.nlm.nih.gov/pubmed/9425143>
37
38 995 100. Costa JM, Grant OM, Chaves MM, I D, M F, RD J, et al. Thermography to explore
39
40 996 plant-environment interactions. J. Exp. Bot. [Internet]. Oxford University Press; 2013
41
42 997 [cited 2017 Jan 24];64:3937–49. Available from: [https://academic.oup.com/jxb/article-](https://academic.oup.com/jxb/article-lookup/doi/10.1093/jxb/ert029)
43
44 998 [lookup/doi/10.1093/jxb/ert029](https://academic.oup.com/jxb/article-lookup/doi/10.1093/jxb/ert029)
45
46 999 101. Zia S, Romano G, Spreer W, Sanchez C, Cairns J, Araus JL, et al. Infrared Thermal
47
48 1000 Imaging as a Rapid Tool for Identifying Water-Stress Tolerant Maize Genotypes of
49
50 1001 Different Phenology. J. Agron. Crop Sci. [Internet]. 2013 [cited 2017 May 12];199:75–
51
52 1002 84. Available from: <http://doi.wiley.com/10.1111/j.1439-037X.2012.00537.x>
53
54 1003 102. Jones HG, Serraj R, Loveys BR, Xiong L, Wheaton A, Price AH. Thermal infrared
55
56 1004 imaging of crop canopies for the remote diagnosis and quantification of plant
57
58 1005 responses to water stress in the field. Funct. Plant Biol. [Internet]. CSIRO PUBLISHING;
59
60 1006 2009 [cited 2017 May 12];36:978. Available from:
61
62 1007 <http://www.publish.csiro.au/?paper=FP09123>
63
64
65

1008 103. Jones HG, Stoll M, Santos T, de Sousa C, Chaves MM, Grant OM. Use of infrared
1009 thermography for monitoring stomatal closure in the field: application to grapevine. J.
1010 Exp. Bot. Oxford University Press; 2002;53:2249–60.

1011 104. Prashar A, Jones H. Infra-Red Thermography as a High-Throughput Tool for Field
1012 Phenotyping. Agronomy [Internet]. Multidisciplinary Digital Publishing Institute; 2014
1013 [cited 2017 May 21];4:397–417. Available from: [http://www.mdpi.com/2073-
1014 4395/4/3/397/](http://www.mdpi.com/2073-4395/4/3/397/)

1015 105. Mahlein A-K. Precision agriculture and plant phenotyping are information-and
1016 technology-based domains with specific demands and challenges for. Plant Dis.
1017 [Internet]. Plant Disease; 2016 [cited 2017 Jan 18];100:241–51. Available from:
1018 <http://apsjournals.apsnet.org/doi/10.1094/PDIS-03-15-0340-FE>

1019 106. Oerke E-C, Fröhling P, Steiner U. Thermographic assessment of scab disease on
1020 apple leaves. Precis. Agric. [Internet]. Springer US; 2011 [cited 2017 May 21];12:699–
1021 715. Available from: <http://link.springer.com/10.1007/s11119-010-9212-3>

1022 107. Chapple CC, Vogt T, Ellis BE, Somerville CR. An Arabidopsis mutant defective in the
1023 general phenylpropanoid pathway. Plant Cell [Internet]. American Society of Plant
1024 Biologists; 1992 [cited 2017 Jun 13];4:1413–24. Available from:
1025 <http://www.ncbi.nlm.nih.gov/pubmed/1477555>

1026 108. Gould PD, Diaz P, Hogben C, Kusakina J, Salem R, Hartwell J, et al. Delayed
1027 fluorescence as a universal tool for the measurement of circadian rhythms in higher
1028 plants. Plant J. [Internet]. 2009 [cited 2011 Jul 15];58:893–901. Available from:
1029 <http://www.ncbi.nlm.nih.gov/pubmed/19638147>

1030 109. Sweeney BM, Prezelin BB, Wong D, Govindjee. In vivo Chlorophyll-a Fluorescence
1031 Transients and the Circadian-Rhythm of Photosynthesis in Gonyaulax-Polyedra.
1032 Photochem. Photobiol. 1979;30:309–11.

1033 110. Sheehan H, Moser M, Klahre U, Esfeld K, Dell’Olivo A, Mandel T, et al. MYB-FL
1034 controls gain and loss of floral UV absorbance, a key trait affecting pollinator
1035 preference and reproductive isolation. Nat. Genet. [Internet]. 2015; Available from:
1036 <http://www.nature.com/doi/10.1038/ng.3462>

1037 111. Pérez-Bueno ML, Pineda M, Cabeza FM, Barón M. Multicolor Fluorescence
1038 Imaging as a Candidate for Disease Detection in Plant Phenotyping. Front. Plant Sci.
1039 [Internet]. Frontiers Media SA; 2016 [cited 2017 Jan 24];7:1790. Available from:

1040 <http://www.ncbi.nlm.nih.gov/pubmed/27994607>

1
2 1041 112. Fang Y, Ramasamy R. Current and Prospective Methods for Plant Disease
3
4 1042 Detection. Biosensors [Internet]. Multidisciplinary Digital Publishing Institute; 2015
5
6 1043 [cited 2017 May 21];5:537–61. Available from: [http://www.mdpi.com/2079-](http://www.mdpi.com/2079-6374/5/3/537/)
7
8 1044 [6374/5/3/537/](http://www.mdpi.com/2079-6374/5/3/537/)

9
10 1045 113. Boviki A. HANDBOOK OF IMAGE AND VIDEO PROCESSING.

11
12 1046 114. Zhang Y, Wang S, Sun P. Pathological brain detection based on wavelet entropy
13
14 1047 and Hu moment invariants. Bio-medical Mater. [Internet]. 2015 [cited 2016 Oct 18];
15
16 1048 Available from: [http://content.iospress.com/articles/bio-medical-materials-and-](http://content.iospress.com/articles/bio-medical-materials-and-engineering/bme1426)
17
18 1049 [engineering/bme1426](http://content.iospress.com/articles/bio-medical-materials-and-engineering/bme1426)

19
20 1050 115. Borisjuk L, Rolletschek H, Neuberger T. Surveying the plant's world by magnetic
21
22 1051 resonance imaging [Internet]. Plant J. 2012 [cited 2017 May 15]. p. 129–46. Available
23
24 1052 from: <http://doi.wiley.com/10.1111/j.1365-3113X.2012.04927.x>

25
26 1053 116. Rascher U, Blossfeld S, Fiorani F, Jahnke S, Jansen M, Kuhn AJ, et al. Non-invasive
27
28 1054 approaches for phenotyping of enhanced performance traits in bean. *Funct. Plant Biol.*
29
30 1055 2011;38:968–83.

31
32 1056 117. Horigane A, Engelaar W, Maruyama S. Visualisation of moisture distribution
33
34 1057 during development of rice caryopses (*Oryza sativa* L.) by nuclear magnetic resonance
35
36 1058 microimaging. *J. Cereal Sci.* [Internet]. 2001 [cited 2017 May 15]; Available from:
37
38 1059 <http://www.sciencedirect.com/science/article/pii/S0733521000903485>

39
40 1060 118. Glidewell S. NMR imaging of developing barley grains. *J. Cereal Sci.* [Internet].
41
42 1061 2006 [cited 2017 May 15]; Available from:
43
44 1062 <http://www.sciencedirect.com/science/article/pii/S0733521005000913>

45
46 1063 119. Converse A, Ahlers E, Bryan T. Positron emission tomography (PET) of radiotracer
47
48 1064 uptake and distribution in living plants: methodological aspects. *Radioanal. ...*
49
50 1065 [Internet]. 2013 [cited 2017 May 15]; Available from:
51
52 1066 <http://link.springer.com/article/10.1007/s10967-012-2383-9>

53
54 1067 120. Karve AA, Alexoff D, Kim D, Schueller MJ, Ferrieri RA, Babst BA. In vivo
55
56 1068 quantitative imaging of photoassimilate transport dynamics and allocation in large
57
58 1069 plants using a commercial positron emission tomography (PET) scanner. *BMC Plant*
59
60 1070 *Biol.* [Internet]. 2015 [cited 2017 May 15];15:273. Available from:
61
62 1071 <http://www.biomedcentral.com/1471-2229/15/273>

- 1072 121. Yang W, Xu X, Duan L, Luo Q, Chen S, Zeng S, et al. High-throughput measurement
1073 of rice tillers using a conveyor equipped with x-ray computed tomography. *Rev. Sci.*
1074 *Instrum.* [Internet]. 2011 [cited 2017 May 15];82:25102. Available from:
1075 <http://aip.scitation.org/doi/10.1063/1.3531980>
- 1076 122. Tracy SR, Roberts JA, Black CR, McNeill A, Davidson R, Mooney SJ. The X-factor:
1077 Visualizing undisturbed root architecture in soils using X-ray computed tomography. *J.*
1078 *Exp. Bot.* 2010;61:311–3.
- 1079 123. Mooney SJ, Pridmore TP, Helliwell J, Bennett MJ. Developing X-ray computed
1080 tomography to non-invasively image 3-D root systems architecture in soil. *Plant Soil.*
1081 2012;352:1–22.
- 1082 124. Metzner R, Eggert A, van Dusschoten D, Pflugfelder D, Gerth S, Schurr U, et al.
1083 Direct comparison of MRI and X-ray CT technologies for 3D imaging of root systems in
1084 soil: potential and challenges for root trait quantification. *Plant Methods* [Internet].
1085 2015 [cited 2017 May 15];11:17. Available from:
1086 <http://www.plantmethods.com/content/11/1/17>
- 1087 125. Lontoc-Roy M, Dutilleul P, Prasher SO, Han L, Brouillet T, Smith DL. Advances in
1088 the acquisition and analysis of CT scan data to isolate a crop root system from the soil
1089 medium and quantify root system complexity in 3-D space. *Geoderma* [Internet]. 2006
1090 [cited 2017 May 16];137:231–41. Available from:
1091 <http://www.sciencedirect.com/science/article/pii/S0016706106002576>
- 1092 126. Perret JS, Al-Belushi ME, Deadman M. Non-destructive visualization and
1093 quantification of roots using computed tomography. *Soil Biol. Biochem.* [Internet].
1094 2007 [cited 2017 May 16];39:391–9. Available from:
1095 <http://www.sciencedirect.com/science/article/pii/S003807170600321X>
- 1096 127. Staedler YM, Masson D, Schönenberger J, Fischer G, Comes H. Plant Tissues in 3D
1097 via X-Ray Tomography: Simple Contrasting Methods Allow High Resolution Imaging.
1098 Sun M, editor. *PLoS One* [Internet]. Public Library of Science; 2013 [cited 2017 May
1099 16];8:e75295. Available from: <http://dx.plos.org/10.1371/journal.pone.0075295>
- 1100 128. Dhondt S, Vanhaeren H, Van Loo D, Cnudde V, Inzé D. Plant structure visualization
1101 by high-resolution X-ray computed tomography. *Trends Plant Sci.* [Internet]. 2010
1102 [cited 2017 May 16];15:419–22. Available from:
1103 <http://www.sciencedirect.com/science/article/pii/S1360138510000956>

1104 129. Brodersen CR, Roddy AB. New frontiers in the three-dimensional visualization of
1 1105 plant structure and function. *Am. J. Bot.* [Internet]. Botanical Society of America; 2016
2
3 1106 [cited 2017 May 16];103:184–8. Available from:
4
5 1107 <http://www.ncbi.nlm.nih.gov/pubmed/26865119>
6
7 1108 130. Jan Erik Solem. *Programming Computer Vision with Python*. Andy Oram, Mike
8
9 1109 Hendrikosn, editors. *Program. Comput. Vis. with Python* [Internet]. 1st ed. Sebastopol:
10
11 1110 O’Reilly Media; 2012;264. Available from: <http://programmingcomputervision.com/>
12
13 1111 131. Navarro PJ, Pérez F, Weiss J, Egea-Cortines M. Machine learning and computer
14
15 1112 vision system for phenotype data acquisition and analysis in plants. *Sensors*
16
17 1113 (Switzerland) [Internet]. Multidisciplinary Digital Publishing Institute; 2016 [cited 2016
18
19 1114 Sep 21];16:1–12. Available from: <http://www.mdpi.com/1424-8220/16/5/641>
20
21 1115 132. Hamuda E, Glavin M, Jones E. A survey of image processing techniques for plant
22
23 1116 extraction and segmentation in the field [Internet]. *Comput. Electron. Agric.* 2016
24
25 1117 [cited 2017 May 10]. p. 184–99. Available from:
26
27 1118 <http://www.sciencedirect.com/science/article/pii/S0168169916301557>
28
29 1119 133. Krig S. *Computer vision metrics: Survey, Taxonomy, and Analysis*. Weiss S, Douglas
30
31 1120 S, editors. ApressOpen; 2014.
32
33 1121 134. Wang Z, Li H, Zhu Y, Xu T. Review of Plant Identification Based on Image
34
35 1122 Processing. *Arch. Comput. Methods Eng.* [Internet]. 2016 [cited 2017 May 10];
36
37 1123 Available from: <http://link.springer.com/10.1007/s11831-016-9181-4>
38
39 1124 135. Bhagwat R, Dandawate Y. Indian plant species identification under varying
40
41 1125 illumination and viewpoint conditions. *2016 Conf. Adv. Signal Process.* [Internet]. IEEE;
42
43 1126 2016 [cited 2017 May 9]. p. 469–73. Available from:
44
45 1127 <http://ieeexplore.ieee.org/document/7746217/>
46
47 1128 136. Thangadurai K, Padmavathi K. Computer vision image enhancement for plant
48
49 1129 leaves disease detection. *Proc. - 2014 World Congr. Comput. Commun. Technol.*
50
51 1130 WCCCT 2014 [Internet]. IEEE; 2014 [cited 2017 May 10]. p. 173–5. Available from:
52
53 1131 <http://ieeexplore.ieee.org/document/6755131/>
54
55 1132 137. Padmavathi K, Thangadurai K. Implementation of RGB and grayscale images in
56
57 1133 plant leaves disease detection - Comparative study. *Indian J. Sci. Technol.* [Internet].
58
59 1134 2016 [cited 2017 May 20];9. Available from:
60
61 1135 <http://www.indjst.org/index.php/indjst/article/view/77739>
62
63
64
65

1 1136 138. Wilkinson MD, Dumontier M, Aalbersberg IJ, Appleton G, Axton M, Baak A, et al.
2 1137 The FAIR Guiding Principles for scientific data management and stewardship. *Sci. Data*
3
4 1138 [Internet]. 2016;3:160018. Available from:
5
6 1139 [http://www.pubmedcentral.nih.gov/articlerender.fcgi?artid=4792175&tool=pmcentre](http://www.pubmedcentral.nih.gov/articlerender.fcgi?artid=4792175&tool=pmcentrez&rendertype=abstract)
7
8 1140 [z&rendertype=abstract](http://www.pubmedcentral.nih.gov/articlerender.fcgi?artid=4792175&tool=pmcentrez&rendertype=abstract)
9
10 1141 139. Singh V, Misra AK. Detection of plant leaf diseases using image segmentation and
11 1142 soft computing techniques. *Inf. Process. Agric.* [Internet]. 2017 [cited 2017 May
12
13 1143 30];4:41–9. Available from:
14
15 1144 <http://www.sciencedirect.com/science/article/pii/S2214317316300154>
16
17 1145 140. Zhao ZQ, Ma LH, Cheung Y ming, Wu X, Tang Y, Chen CLP. ApLeaf: An efficient
18 1146 android-based plant leaf identification system. *Neurocomputing* [Internet]. 2015 [cited
19
20 1147 2017 May 30];151:1112–9. Available from:
21
22 1148 <http://www.sciencedirect.com/science/article/pii/S0925231214013368>
23
24 1149 141. Otsu N. A Threshold Selection Method from Gray-Level Histograms. *IEEE Trans.*
25 1150 *Syst. Man. Cybern.* [Internet]. 1979 [cited 2017 May 30];9:62–6. Available from:
26
27 1151 <http://ieeexplore.ieee.org/document/4310076/>
28
29 1152 142. Liu J-C, Lin T-M. Location and Image-Based Plant Recognition and Recording
30 1153 System. 2015 [cited 2017 May 30];6. Available from:
31
32 1154 <http://www.jihmsp.org/~jihmsp/2015/vol6/JIH-MSP-2015-05-007.pdf>
33
34 1155 143. Chéné Y, Rousseau D, Belin É tienn., Garbez M, Galopin G, Chapeau-Blondeau F.
35 1156 Shape descriptors to characterize the shoot of entire plant from multiple side views of
36 1157 a motorized depth sensor. *Mach. Vis. Appl.* [Internet]. Springer Berlin Heidelberg; 2016
37
38 1158 May 19 [cited 2017 May 30];1–15. Available from:
39
40 1159 <http://link.springer.com/10.1007/s00138-016-0762-x>
41
42 1160 144. Vincent L, Vincent L, Soille P. Watersheds in Digital Spaces: An Efficient Algorithm
43 1161 Based on Immersion Simulations. *IEEE Trans. Pattern Anal. Mach. Intell.* [Internet].
44 1162 1991 [cited 2017 May 30];13:583–98. Available from:
45
46 1163 <http://ieeexplore.ieee.org/document/87344/>
47
48 1164 145. Patil S, Soma S, Nandyal S. Identification of Growth Rate of Plant based on leaf
49 1165 features using Digital Image Processing Techniques. *Int. J. Emerg. Technol. Adv. Eng.*
50 1166 Website www.ijetae.com ISO Certif. J. 2013;3.
51
52 1167 146. Barnes C, Balzter H, Barrett K, Eddy J, Milner S, Suárez J. Individual Tree Crown
53
54
55
56
57
58
59
60
61
62
63
64
65

1 1168 Delineation from Airborne Laser Scanning for Diseased Larch Forest Stands. Remote
2 1169 Sens. [Internet]. Multidisciplinary Digital Publishing Institute; 2017 [cited 2017 Apr
3 1170 24];9:231. Available from: <http://www.mdpi.com/2072-4292/9/3/231>
4 1171 147. Vukadinovic D, Polder G. Watershed and supervised classification based fully
5 1172 automated method for separate leaf segmentation. COST FA 1306 -The quest Toler.
6 1173 Var. plant Cell. Lev. Gatersleben; 2015.
7 1174 148. Rother C, Kolmogorov V, Blake A. GrabCut -Interactive Foreground Extraction
8 1175 using Iterated Graph Cuts. ACM Trans. Graph. [Internet]. 2004. Available from:
9 1176 [https://www.microsoft.com/en-us/research/publication/grabcut-interactive-](https://www.microsoft.com/en-us/research/publication/grabcut-interactive-foreground-extraction-using-iterated-graph-cuts/)
10 1177 [foreground-extraction-using-iterated-graph-cuts/](https://www.microsoft.com/en-us/research/publication/grabcut-interactive-foreground-extraction-using-iterated-graph-cuts/)
11 1178 149. Boykov YY, Jolly M-P. Interactive graph cuts for optimal boundary & region
12 1179 segmentation of objects in N-D images. Proc. Eighth IEEE Int. Conf. Comput. Vision.
13 1180 ICCV 2001 [Internet]. IEEE Comput. Soc; 2001 [cited 2016 Nov 3]. p. 105–12. Available
14 1181 from: <http://ieeexplore.ieee.org/document/937505/>
15 1182 150. Sonka M, Hlavac V, Boyle R. Image Processing, Analysis, and Machine Vision. 3rd
16 1183 ed. Thomson, editor. Toronto: Thomson; 2008.
17 1184 151. Wang X. The GrabCut Segmentation Technique as Used in the Study of Tree Image
18 1185 Extraction. In: Zhu FG and X, editor. Proc. 2009 Int. Work. Inf. Secur. Appl. (IWISA
19 1186 2009). Qingdao, China: Academy Publisher; 2009.
20 1187 152. Liu J-C, Chiang C-Y, Chen S. Image-Based Plant Recognition by Fusion of
21 1188 Multimodal Information. 2016 10th Int. Conf. Innov. Mob. Internet Serv. Ubiquitous
22 1189 Comput. [Internet]. IEEE; 2016 [cited 2017 May 30]. p. 5–11. Available from:
23 1190 <http://ieeexplore.ieee.org/document/7794433/>
24 1191 153. Liu J-C, Lin T-M. Location and Image-Based Plant Recognition and Recording
25 1192 System. 2015;6. Available from: [http://www.jihmsp.org/~jihmsp/2015/vol6/JIH-MSP-](http://www.jihmsp.org/~jihmsp/2015/vol6/JIH-MSP-2015-05-007.pdf)
26 1193 [2015-05-007.pdf](http://www.jihmsp.org/~jihmsp/2015/vol6/JIH-MSP-2015-05-007.pdf)
27 1194 154. Kass M, Witkin A, Terzopoulos D. Snakes: Active contour models. Int. J. Comput.
28 1195 Vis. [Internet]. Kluwer Academic Publishers; 1988 [cited 2016 Nov 5];1:321–31.
29 1196 Available from: <http://link.springer.com/10.1007/BF00133570>
30 1197 155. Minervini M, Abdelsamea MM, Tsafaris SA. Image-based plant phenotyping with
31 1198 incremental learning and active contours. Ecol. Inform. 2014;23:35–48.
32 1199 156. Suta L, Bessy F, Veja C, Vaida M-F. Active contours: Application to plant

1 1200 recognition. 2012 IEEE 8th Int. Conf. Intell. Comput. Commun. Process. [Internet]. IEEE;
2 1201 2012 [cited 2016 Nov 5]. p. 181–7. Available from:
3
4 1202 <http://ieeexplore.ieee.org/document/6356183/>
5
6 1203 157. Shi Y, Karl WC. A real-time algorithm for the approximation of level-set-based
7
8 1204 curve evolution. IEEE Trans. Image Process. [Internet]. 2008 [cited 2016 Nov
9
10 1205 5];17:645–56. Available from: <http://ieeexplore.ieee.org/document/4480128/>
11
12 1206 158. Chan TF, Vese LA. Active contours without edges. IEEE Trans. Image Process.
13
14 1207 [Internet]. IEEE Press; 2001 [cited 2016 Nov 5];10:266–77. Available from:
15
16 1208 <http://ieeexplore.ieee.org/document/902291/>
17
18 1209 159. Pape J-M, Klukas C. Utilizing machine learning approaches to improve the
19
20 1210 prediction of leaf counts and individual leaf segmentation of rosette plant images.
21
22 1211 Proc. Comput. Vis. Probl. Plant Phenotyping [Internet]. British Machine Vision
23
24 1212 Association; 2015 [cited 2016 Sep 21];1–12. Available from:
25
26 1213 <http://www.bmva.org/bmvc/2015/cvppp/papers/paper003/index.html>
27
28 1214 160. Arivazhagan S, Shebiah RN, Ananthi S, Vishnu Varthini S. Detection of unhealthy
29
30 1215 region of plant leaves and classification of plant leaf diseases using texture features.
31
32 1216 Agric. Eng. Int. CIGR J. 2013;15:211–7.
33
34 1217 161. Mouille G, Robin S, Lecomte M, Pagant S, Höfte H. Classification and identification
35
36 1218 of *Arabidopsis* cell wall mutants using Fourier-Transform InfraRed (FT-IR)
37
38 1219 microspectroscopy. Plant J. [Internet]. Blackwell Science Ltd; 2003 [cited 2017 May
39
40 1220 27];35:393–404. Available from: <http://doi.wiley.com/10.1046/j.1365->
41
42 1221 [313X.2003.01807.x](http://doi.wiley.com/10.1046/j.1365-313X.2003.01807.x)
43
44 1222 162. Guijarro M, Riomoros I, Pajares G, Zitinski P. Discrete wavelets transform for
45
46 1223 improving greenness image segmentation in agricultural images. Comput. Electron.
47
48 1224 Agric. 2015;118:396–407.
49
50 1225 163. Iyer-Pascuzzi AS, Symonova O, Mileyko Y, Hao Y, Belcher H, Harer J, et al. Imaging
51
52 1226 and analysis platform for automatic phenotyping and trait ranking of plant root
53
54 1227 systems. Plant Physiol. [Internet]. American Society of Plant Biologists; 2010 [cited
55
56 1228 2017 May 28];152:1148–57. Available from:
57
58 1229 <http://www.ncbi.nlm.nih.gov/pubmed/20107024>
59
60 1230 164. Lowe DG. Distinctive Image Features from Scale-Invariant Keypoints. Int. J.
61
62 1231 Comput. Vis. [Internet]. Kluwer Academic Publishers; 2004 [cited 2016 Dec 7];60:91–

- 1232 110. Available from: <http://link.springer.com/10.1023/B:VISI.0000029664.99615.94>
- 1233 165. Bay H, Ess A, Tuytelaars T, Van Gool L. Speeded-Up Robust Features (SURF).
1234 Comput. Vis. Image Underst. 2008;110:346–59.
- 1235 166. Dalal N, Triggs B. Histograms of Oriented Gradients for Human Detection. 2005
1236 IEEE Comput. Soc. Conf. Comput. Vis. Pattern Recognit. [Internet]. IEEE; [cited 2016
1237 Dec 9]. p. 886–93. Available from: <http://ieeexplore.ieee.org/document/1467360/>
- 1238 167. Guo W, Fukatsu T, Ninomiya S. Automated characterization of flowering dynamics
1239 in rice using field-acquired time-series RGB images. Plant Methods [Internet]. 2015
1240 [cited 2017 May 28];11:7. Available from:
1241 <http://www.plantmethods.com/content/11/1/7>
- 1242 168. Santos T, Oliveira A. Image-based 3D digitizing for plant architecture analysis and
1243 phenotyping. ... SIBGRAPI 2012 (XXV Conf. ... [Internet]. 2012 [cited 2016 Dec 8];
1244 Available from: http://www.cnptia.embrapa.br/~thiago/pool/2012-08-24_sibgrapi.pdf
- 1245 169. Roscher R, Herzog K, Kunkel A, Kicherer A, Töpfer R, Frestner W. Automated
1246 image analysis framework for high-throughput determination of grapevine berry sizes
1247 using conditional random fields. Comput. Electron. Agric. [Internet]. 2014 [cited 2017
1248 May 29];100:148–58. Available from:
1249 <http://www.sciencedirect.com/science/article/pii/S0168169913002780>
- 1250 170. Lantz B. Machine Learning with R. 1st ed. Jones J, Sheikh A, editors. Birmingham:
1251 Packt Publishing; 2013.
- 1252 171. Müller A, Guido S. Introduction to Machine Learning with Python. 1st ed.
1253 Schanafelt D, editor. Sebastopol: O'Reilly Media; 2016.
- 1254 172. Smola A, Vishwanathan SV. Introduction to Machine Learning. 1st ed. Cambridge:
1255 Cambridge University Press; 2008.
- 1256 173. Baranowski P, Jedryczka M, Mazurek W, Babula-Skowronska D, Siedliska A,
1257 Kaczmarek J. Hyperspectral and thermal imaging of oilseed rape (*Brassica napus*)
1258 response to fungal species of the genus *Alternaria*. Wilson RA, editor. PLoS One
1259 [Internet]. Public Library of Science; 2015 [cited 2016 Nov 6];10:e0122913. Available
1260 from: <http://dx.plos.org/10.1371/journal.pone.0122913>
- 1261 174. Fukushima K. Neocognitron: a self organizing neural network model for a
1262 mechanism of pattern recognition unaffected by shift in position. Biol. Cybern.
1263 [Internet]. 1980 [cited 2016 Nov 6];36:193–202. Available from:

1264 <http://www.ncbi.nlm.nih.gov/pubmed/7370364>

1265 175. Pound MP, Burgess AJ, Wilson MH, Atkinson JA, Griffiths M, Jackson AS, et al.

1266 Deep Machine Learning provides state-of-the-art performance in image-based plant

1267 phenotyping. *bioRxiv* [Internet]. 2016 [cited 2016 Sep 21];53033. Available from:

1268 <http://biorxiv.org/lookup/doi/10.1101/053033>

1269 176. Mohanty SP, Hughes D, Salathé M. Using Deep Learning for Image-Based Plant

1270 Disease Detection. 2016;1–7.

1271 177. Tsafaris SA, Minervini M, Scharr H. Machine Learning for Plant Phenotyping

1272 Needs Image Processing [Internet]. *Trends Plant Sci.* 2016 [cited 2017 May 27]. p. 989–

1273 91. Available from: <http://linkinghub.elsevier.com/retrieve/pii/S1360138516301613>

1274 178. Naik HS, Zhang J, Lofquist A, Assefa T, Sarkar S, Ackerman D, et al. A real-time

1275 phenotyping framework using machine learning for plant stress severity rating in

1276 soybean. *Plant Methods* [Internet]. 2017 [cited 2017 May 29];13:23. Available from:

1277 <http://plantmethods.biomedcentral.com/articles/10.1186/s13007-017-0173-7>

1278 179. Nagler PL, Inoue Y, Glenn E., Russ A., Daughtry CS. Cellulose absorption index

1279 (CAI) to quantify mixed soil–plant litter scenes. *Remote Sens. Environ.* 2003;87:310–

1280 25.

1281 180. Ren H, Zhou G, Zhang F, Zhang X. Evaluating cellulose absorption index (CAI) for

1282 non-photosynthetic biomass estimation in the desert steppe of Inner Mongolia.

1283 *Chinese Sci. Bull.* SP Science China Press; 2012;57:1716–22.

1284 181. Serbin G, Daughtry CST, Hunt ER, Reeves JB, Brown DJ. Effects of soil composition

1285 and mineralogy on remote sensing of crop residue cover. *Remote Sens. Environ.*

1286 2009;113:224–38.

1287 182. Eskandari I, Navid H, Rangzan K. Evaluating spectral indices for determining

1288 conservation and conventional tillage systems in a vetch-wheat rotation. *Int. Soil*

1289 *Water Conserv. Res.* 2016;4:93–8.

1290 183. Galvão LS, Formaggio AR, Tisot DA. Discrimination of sugarcane varieties in

1291 Southeastern Brazil with EO-1 Hyperion data. *Remote Sens. Environ.* 2005;94:523–34.

1292 184. Price J. Leaf area index estimation from visible and near-infrared reflectance data.

1293 *Remote Sens. Environ.* 1995;52:55–65.

1294 185. Zarco-Tejada P, Berjón A, Miller J. Stress detection in crops with hyperspectral

1295 remote sensing and physical simulation models. *Proc. Airborne.* 2004;

1296 186. Cai J, Golzarian MR, Miklavcic SJ. Novel Image Segmentation Based on Machine
1297 Learning and Its Application to Plant Analysis. *Int. J. Inf. Electron. Eng.* 2011;1.
1298 187. Gong P, Pu R, Biging G. Estimation of forest leaf area index using vegetation
1299 indices derived from Hyperion hyperspectral data. *IEEE Trans.* 2003;
1300 188. Brown HE, Diuk-Wasser MA, Guan Y, Caskey S, Fish D. Comparison of three
1301 satellite sensors at three spatial scales to predict larval mosquito presence in
1302 Connecticut wetlands. *Remote Sens. Environ.* 2008;112:2301–8.
1303 189. Apan A, Held A, Phinn S, Markley J. Detecting sugarcane “orange rust” disease
1304 using EO-1 Hyperion hyperspectral imagery. *Int. J. Remote Sens.* Taylor & Francis
1305 Group ; 2004;25:489–98.
1306 190. Tucker CJ, Slayback DA, Pinzon JE, Los SO, Myneni RB, Taylor MG. Higher northern
1307 latitude normalized difference vegetation index and growing season trends from 1982
1308 to 1999. *Int. J. Biometeorol.* Springer-Verlag; 2001;45:184–90.
1309 191. Haboudane D, Miller JR, Pattey E, Zarco-Tejada PJ, Strachan IB. Hyperspectral
1310 vegetation indices and novel algorithms for predicting green LAI of crop canopies:
1311 Modeling and validation in the context of precision agriculture. *Remote Sens. Environ.*
1312 2004;90:337–52.
1313 192. Pagani A, Echeverría HE, Andrade FH, Sainz Rozas HR. Characterization of Corn
1314 Nitrogen Status with a Greenness Index under Different Availability of Sulfur. *Agron. J.*
1315 American Society of Agronomy; 2009;101:315.
1316 193. Blackburn GA. Spectral indices for estimating photosynthetic pigment
1317 concentrations: A test using senescent tree leaves. *Int. J. Remote Sens.* Taylor &
1318 Francis Group ; 1998;19:657–75.
1319 194. Hunt ER, Dean Hively W, Fujikawa SJ, Linden DS, Daughtry CST, McCarty GW.
1320 Acquisition of NIR-green-blue digital photographs from unmanned aircraft for crop
1321 monitoring. *Remote Sens. Molecular Diversity Preservation International*; 2010;2:290–
1322 305.
1323 195. Bell GE, Howell BM, Johnson GV, Raun WR, Solie JB, Stone ML. Optical Sensing of
1324 Turfgrass Chlorophyll Content and Tissue Nitrogen. *HortScience.* American Society for
1325 Horticultural Science; 2004;39:1130–2.
1326 196. Haboudane D, Miller JR, Tremblay N, Zarco-Tejada PJ, Dextraze L. Integrated
1327 narrow-band vegetation indices for prediction of crop chlorophyll content for

- 1328 application to precision agriculture. *Remote Sens. Environ.* 2002;81:416–26.
- 1329 197. Timm BC, McGarigal K. Fine-scale remotely-sensed cover mapping of coastal dune
1330 and salt marsh ecosystems at Cape Cod National Seashore using Random Forests.
1331 *Remote Sens. Environ.* 2012;127:106–17.
- 1332 198. Parenteau MP, Bannari A, El-Harti A, Bachaoui M, El-Ghmari A. Characterization of
1333 the state of soil degradation by erosion using the hue and coloration indices. *IGARSS*
1334 2003. 2003 IEEE Int. Geosci. Remote Sens. Symp. Proc. (IEEE Cat. No.03CH37477). IEEE;
1335 p. 2284–6.
- 1336 199. Pajares G, Ruz JJ, de la Cruz JM. Performance analysis of homomorphic systems
1337 for image change detection. *Pattern Recognit. Image Anal. Pt 1* [Internet]. Springer,
1338 Berlin, Heidelberg; 2005 [cited 2017 Jul 25]. p. 563–70. Available from:
1339 http://link.springer.com/10.1007/11492429_68
- 1340 200. Perez AJ, Lopez F, Benlloch J V., Christensen S. Colour and shape analysis
1341 techniques for weed detection in cereal fields. *Comput. Electron. Agric.* [Internet].
1342 2000 [cited 2017 Jul 25];25:197–212. Available from:
1343 <http://linkinghub.elsevier.com/retrieve/pii/S016816999900068X>
- 1344 201. Oluleye B, Leisa A, Jinsong L, Dean D. On the Application of Genetic Probabilistic
1345 Neural Networks and Cellular Neural Networks in Precision Agriculture. *Asian J.*
1346 *Comput. Inf. Syst.* [Internet]. 2014 [cited 2017 Aug 8];2:90–101. Available from:
1347 <http://ro.ecu.edu.au/ecuworkspost2013/677>
- 1348 202. Knoll FJ, Holtorf T, Hussmann S. Modified 3D time-of-flight camera for object
1349 separation in organic farming. In: Kress BC, Osten W, Urbach HP, editors. *International*
1350 *Society for Optics and Photonics*; 2017 [cited 2017 Aug 9]. p. 103351R. Available from:
1351 <http://proceedings.spiedigitallibrary.org/proceeding.aspx?doi=10.1117/12.2270276>
- 1352 203. Huang K-Y. Application of artificial neural network for detecting Phalaenopsis
1353 seedling diseases using color and texture features. *Comput. Electron. Agric.* [Internet].
1354 2007 [cited 2017 Sep 11];57:3–11. Available from:
1355 <http://linkinghub.elsevier.com/retrieve/pii/S0168169907000385>
- 1356 204. Mokhtar U, Ali MAS, Hassanien AE, Hefny H. Identifying Two of Tomatoes Leaf
1357 Viruses Using Support Vector Machine. Springer, New Delhi; 2015 [cited 2017 Sep 11].
1358 p. 771–82. Available from: http://link.springer.com/10.1007/978-81-322-2250-7_77
- 1359 205. Casanova J, O’Shaughnessy S, Evett S, Rush C. Development of a Wireless

1360 Computer Vision Instrument to Detect Biotic Stress in Wheat. *Sensors* [Internet].
1361 Multidisciplinary Digital Publishing Institute; 2014 [cited 2017 Sep 11];14:17753–69.
1362 Available from: <http://www.mdpi.com/1424-8220/14/9/17753/>
1363 206. Bauer SD, Korč F, Förstner W. The potential of automatic methods of classification
1364 to identify leaf diseases from multispectral images. *Precis. Agric.* [Internet]. Springer
1365 US; 2011 [cited 2017 Sep 11];12:361–77. Available from:
1366 <http://link.springer.com/10.1007/s11119-011-9217-6>
1367 207. Atkinson JA, Lobet G, Noll M, Meyer PE, Griffiths M, Wells DM. Combining semi-
1368 automated image analysis techniques with machine learning algorithms to accelerate
1369 large scale genetic studies. *bioRxiv* [Internet]. 2017 [cited 2017 Aug 8]; Available from:
1370 <http://www.biorxiv.org/content/early/2017/06/20/152702>
1371 208. Ballabeni A, Apollonio FI, Gaiani M, Remondino F. Advances in image pre-
1372 processing to improve automated 3d reconstruction. *Int. Arch. Photogramm. Remote*
1373 *Sens. Spat. Inf. Sci. - ISPRS Arch.* [Internet]. 2015 [cited 2017 Jul 20]. p. 315–23.
1374 Available from: [http://www.int-arch-photogramm-remote-sens-spatial-inf-sci.net/XL-
1375 5-W4/315/2015/](http://www.int-arch-photogramm-remote-sens-spatial-inf-sci.net/XL-5-W4/315/2015/)
1376 209. Klodt M, Herzog K, Töpfer R, Cremers D. Field phenotyping of grapevine growth
1377 using dense stereo reconstruction. *BMC Bioinformatics* [Internet]. BioMed Central;
1378 2015 [cited 2017 Jul 20];16:143. Available from:
1379 <http://www.ncbi.nlm.nih.gov/pubmed/25943369>
1380 210. Zhang X, Huang C, Wu D, Qiao F, Li W, Duan L, et al. High-throughput phenotyping
1381 and QTL mapping reveals the genetic architecture of maize plant growth. *Plant Physiol.*
1382 [Internet]. 2017;pp.01516.2016. Available from:
1383 <http://www.plantphysiol.org/lookup/doi/10.1104/pp.16.01516>
1384 211. Tsung-Shiang H. An Improvement Stereo Vision Images Processing for Object
1385 Distance Measurement. *Int. J. Autom. Smart Technol.* [Internet]. 2015 [cited 2017 Aug
1386 9];5:85–90. Available from:
1387 <http://www.ausmt.org/index.php/AUSMT/article/view/460>
1388 212. Raza SEA, Smith HK, Clarkson GJJ, Taylor G, Thompson AJ, Clarkson J, et al.
1389 Automatic detection of regions in spinach canopies responding to soil moisture deficit
1390 using combined visible and thermal imagery. Merks RMH, editor. *PLoS One* [Internet].
1391 Public Library of Science; 2014 [cited 2017 Aug 9];9:e97612. Available from:

1392 <http://dx.plos.org/10.1371/journal.pone.0097612>

1393 213. Raza SEA, Prince G, Clarkson JP, Rajpoot NM. Automatic detection of diseased
1394 tomato plants using thermal and stereo visible light images. Perovic D, editor. PLoS
1395 One [Internet]. Narosa Publishing House; 2015 [cited 2017 Aug 9];10:e0123262.
1396 Available from: <http://dx.plos.org/10.1371/journal.pone.0123262>

1397 214. Kazmi W, Foix S, Alenyà G, Andersen HJ. Indoor and outdoor depth imaging of
1398 leaves with time-of-flight and stereo vision sensors: Analysis and comparison. ISPRS J.
1399 Photogramm. Remote Sens. [Internet]. 2014 [cited 2017 Aug 9];88:128–46. Available
1400 from: <http://linkinghub.elsevier.com/retrieve/pii/S0924271613002748>

1401 215. Wahabzada M, Mahlein A-K, Bauckhage C, Steiner U, Oerke E-C, Kersting K. Plant
1402 Phenotyping using Probabilistic Topic Models: Uncovering the Hyperspectral Language
1403 of Plants. Sci. Rep. [Internet]. Nature Publishing Group; 2016 [cited 2016 Oct
1404 18];6:22482. Available from: <http://www.nature.com/articles/srep22482>

1405 216. Ochoa D, Cevallos J, Vargas G, Criollo R, Romero D, Castro R, et al. Hyperspectral
1406 imaging system for disease scanning on banana plants. Kim MS, Chao K, Chin BA,
1407 editors. Proc. SPIE 9864, Sens. Agric. Food Qual. Saf. VIII [Internet]. International
1408 Society for Optics and Photonics; 2016 [cited 2017 Jul 20];4:98640M. Available from:
1409 <http://proceedings.spiedigitallibrary.org/proceeding.aspx?doi=10.1117/12.2224242>

1410 217. Mahlein A-K, Kuska MT, Thomas S, Bohnenkamp D, Alisaac E, Behmann J, et al.
1411 Plant disease detection by hyperspectral imaging: from the lab to the field. Adv. Anim.
1412 Biosci. [Internet]. 2017 [cited 2017 Jul 20];8:238–43. Available from:
1413 https://www.cambridge.org/core/product/identifier/S2040470017001248/type/journal_article

1414

1415 218. Pandey P, Ge Y, Stoerger V, Schnable JC. High Throughput In vivo Analysis of Plant
1416 Leaf Chemical Properties Using Hyperspectral Imaging. Front. Plant Sci. [Internet].
1417 Frontiers; 2017 [cited 2017 Aug 9];8:1348. Available from:
1418 <http://journal.frontiersin.org/article/10.3389/fpls.2017.01348/full>

1419 219. Wahabzada M, Mahlein AK, Bauckhage C, Steiner U, Oerke EC, Kersting K. Metro
1420 maps of plant disease dynamics-automated mining of differences using hyperspectral
1421 images. Lightfoot DA, editor. PLoS One [Internet]. Springer; 2015 [cited 2017 Sep
1422 11];10:e0116902. Available from: <http://dx.plos.org/10.1371/journal.pone.0116902>

1423 220. Chattopadhyay S, Akbar SA, Elfiky NM, Medeiros H, Kak A. Measuring and

1424 modeling apple trees using time-of-flight data for automation of dormant pruning
1 1425 applications. 2016 IEEE Winter Conf. Appl. Comput. Vision, WACV 2016 [Internet].
2 1426 IEEE; 2016 [cited 2017 Sep 4]. p. 1–9. Available from:
3
4 1427 <http://ieeexplore.ieee.org/document/7477596/>
5
6 1428 221. Chéné Y, Rousseau D, Lucidarme P, Bertheloot J, Caffier V, Morel P, et al. On the
7
8 1429 use of depth camera for 3D phenotyping of entire plants. *Comput. Electron. Agric.*
9
10 1430 [Internet]. 2012 [cited 2017 Sep 4];82:122–7. Available from:
11
12 1431 <http://linkinghub.elsevier.com/retrieve/pii/S016816991100319X>
13
14 1432 222. Weiss U, Biber P, Laible S, Bohlmann K, Zell A. Plant species classification using a
15
16 1433 3D LIDAR sensor and machine learning. *Proc. - 9th Int. Conf. Mach. Learn. Appl. ICMLA*
17
18 1434 2010 [Internet]. IEEE; 2010 [cited 2017 Aug 8]. p. 339–45. Available from:
19
20 1435 <http://ieeexplore.ieee.org/document/5708854/>
21
22 1436 223. Greaves HE, Vierling LA, Eitel JUH, Boelman NT, Magney TS, Prager CM, et al.
23
24 1437 Applying terrestrial lidar for evaluation and calibration of airborne lidar-derived shrub
25
26 1438 biomass estimates in Arctic tundra. *Remote Sens. Lett.* [Internet]. Taylor & Francis;
27
28 1439 2017 [cited 2017 Aug 8];8:175–84. Available from:
29
30 1440 <https://www.tandfonline.com/doi/full/10.1080/2150704X.2016.1246770>
31
32 1441 224. Paulus S, Dupuis J, Mahlein A-K, Kuhlmann H. Surface feature based classification
33
34 1442 of plant organs from 3D laserscanned point clouds for plant phenotyping. *BMC*
35
36 1443 *Bioinformatics* [Internet]. 2013 [cited 2017 Sep 11];14:238. Available from:
37
38 1444 <http://bmcbioinformatics.biomedcentral.com/articles/10.1186/1471-2105-14-238>
39
40 1445 225. Liu S, Baret F, Abichou M, Boudon F, Thomas S, Zhao K, et al. Estimating wheat
41
42 1446 green area index from ground-based LiDAR measurement using a 3D canopy structure
43
44 1447 model. *Agric. For. Meteorol.* [Internet]. 2017 [cited 2017 Aug 8];247:12–20. Available
45
46 1448 from: <http://linkinghub.elsevier.com/retrieve/pii/S016819231730223X>
47
48 1449 226. Lopatin J, Dolos K, Hernández HJ, Galleguillos M, Fassnacht FE. Comparing
49
50 1450 Generalized Linear Models and random forest to model vascular plant species richness
51
52 1451 using LiDAR data in a natural forest in central Chile. *Remote Sens. Environ.* [Internet].
53
54 1452 2016 [cited 2017 Aug 8];173:200–10. Available from:
55
56 1453 <http://linkinghub.elsevier.com/retrieve/pii/S0034425715302169>
57
58 1454 227. García-Tejero IF, Hernández A, Padilla-Díaz CM, Diaz-Espejo A, Fernández J.
59
60 1455 Assessing plant water status in a hedgerow olive orchard from thermography at plant
61
62
63
64
65

1456 level. *Agric. Water Manag.* [Internet]. 2017 [cited 2017 Sep 6];188:50–60. Available
1 1457 from: <http://linkinghub.elsevier.com/retrieve/pii/S0378377417301269>
2
3 1458 228. Deery DM, Rebetzke GJ, Jimenez-Berni JA, James RA, Condon AG, Bovill WD, et al.
4 1459 Methodology for High-Throughput Field Phenotyping of Canopy Temperature Using
5 Airborne Thermography. *Front. Plant Sci.* [Internet]. Frontiers Media SA; 2016 [cited
6 1460 2017 Sep 6];7:1808. Available from: <http://www.ncbi.nlm.nih.gov/pubmed/27999580>
7 1461 229. Rousseau C, Belin E, Bove E, Rousseau D, Fabre F, Berruyer R, et al. High
8 1462 throughput quantitative phenotyping of plant resistance using chlorophyll
9 1463 fluorescence image analysis. *Plant Methods* [Internet]. 2013 [cited 2017 Sep 6];9:17.
10 1464 Available from: [http://plantmethods.biomedcentral.com/articles/10.1186/1746-4811-](http://plantmethods.biomedcentral.com/articles/10.1186/1746-4811-9-17)
11 1465 9-17
12 1466 230. Wetterich CB, Felipe de Oliveira Neves R, Belasque J, Ehsani R, Marcassa LG.
13 1467 Detection of Huanglongbing in Florida using fluorescence imaging spectroscopy and
14 1468 machine-learning methods. *Appl. Opt.* [Internet]. Optical Society of America; 2017
15 1469 [cited 2017 Sep 7];56:15. Available from:
16 1470 <https://www.osapublishing.org/abstract.cfm?URI=ao-56-1-15>
17 1471 231. Hillnhutter C, Sikora RA, Oerke E-C, van Dusschoten D. Nuclear magnetic
18 1472 resonance: a tool for imaging belowground damage caused by *Heterodera schachtii*
19 1473 and *Rhizoctonia solani* on sugar beet. *J. Exp. Bot.* [Internet]. Kluwer Academic
20 1474 Publishers, Wageningen, The Netherlands; 2012 [cited 2017 Sep 5];63:319–27.
21 1475 Available from: <https://academic.oup.com/jxb/article-lookup/doi/10.1093/jxb/err273>
22 1476 232. Yang W, Xu X, Duan L, Luo Q, Chen S, Zeng S, et al. High-throughput measurement
23 1477 of rice tillers using a conveyor equipped with x-ray computed tomography. *Rev. Sci.*
24 1478 *Instrum.* [Internet]. American Institute of Physics; 2011 [cited 2017 Sep 5];82:25102.
25 1479 Available from: <http://aip.scitation.org/doi/10.1063/1.3531980>
26 1480 233. Donis-González IR, Guyer DE, Fulbright DW, Pease A. Postharvest noninvasive
27 1481 assessment of fresh chestnut (*Castanea* spp.) internal decay using computer
28 1482 tomography images. *Postharvest Biol. Technol.* [Internet]. 2014 [cited 2017 Sep
29 1483 7];94:14–25. Available from:
30 1484 <http://linkinghub.elsevier.com/retrieve/pii/S0925521414000805>
31 1485
32 1486
33 1487

1488 Tables

1489 Table 1. List of software tools for image processing

Vision libraries	Source	Language
OpenCV EmguCV	http://opencv.org http://www.emgu.com/	C++, Python, Java, C#
PlantCV Scikit-image	http://plantcv.danforthcenter.org http://scikit-image.org	Python
Bioimagetools, bayesimages, edci, DRIP, dpmixsim, raster, ...	https://cran.r-project.org/	R
Cimg Simplecv Fastcv Ccv Vxl	http://cimg.eu http://Simplecv.org https://developer.qualcomm.com/software/fastcv- sdk http://libccv.org http://vxl.sourceforge.net	C++
BoofCV OpenIMAJ JavaCV	http://boofcv.org http://openimaj.org https://github.com/bytedeco/javacv	Java

1490

1491

1492

1493 Table 2. A list of indexes, the corresponding wavelength ranges and their use to analyse
 1494 plant material.

1495

Index	Range nm	Applications
CAI – Cellulose Absorption Index	2200-2000	Quantification mixed soil–plant litter scenes [179], estimation of non-photosynthetic biomass [180]
LCA – Lignin-Cellulose Absorption Index	2365-2145	Measure the effects of soil composition and mineralogy of crop residue cover [181]
NTDI – Normalized Difference Tillage Index	2359-1150	Used for identifying crop residue cover in conventional and conservation tillage systems [182]
LWVI-1 – Normalized Difference Leaf water VI 2	1094-893	Discrimination of sugarcane varieties, allowed to detect large amounts of non photosynthetically-active constituents within the canopy [183]
DLAI – Difference Leaf Area Index	1725-970	Used for estimating leaf area index based on the radiation measurements in the visible and near-infrared [184]
PWI – Plant Water Index	970-902	Water content estimation and study of the characteristics of canopy spectrum and growth status [185][186]
NLI – Nonlinear vegetation index	1400-780	Measurement of plant leaf water content. In combination with others indexes can detect interaction of biochemicals such as protein, nitrogen, lignin, cellulose, sugar, and starch [187]
DWSI – Disease water stress index	1657-547	To predict larval mosquito presence in wetland [188]and detect sugarcane 'orange rust' disease [189]
NDVI – Normalized Difference Vegetation Index	800-670	Measurement significant variations in photosynthetic activity and growing season length at different latitudes [190]
MCARI – Modified Chlorophyll Absorption Ratio Index	700-670	Study of vegetation biophysical parameters, as well as to external factors affecting canopy reflectance [191]
GI – Greenness Index	670-550	Characterization of corn nitrogen status [192]
CAR – Chlorophyll absorption ratio	700-500	Estimating the concentration of individual photosynthetic pigments within vegetation [193]
GNDVI – Green normalized difference vegetation index	800-550	Providing important information for site-specific agricultural decision making [194] and for identification of chlorophyll content and tissue nitrogen [195]
OSAVI – Optimized Soil Adjusted Vegetation Index	800-670	Measurement with high sensitive of chlorophyll content variations and very resistant to the variations of LAI and solar zenith angle [196]
CI r – Coloration Index red	780-710	Mapping of coastal dune and salt marsh ecosystems [197]
CI g – Coloration Index green	780-550	Characterization of the state of soil degradation by erosion [198]

1496

1497

1498

1499

1500

- 1
- 2
- 3
- 4
- 5
- 6
- 7
- 8
- 9
- 10
- 11
- 12
- 13
- 14
- 15
- 16
- 17
- 18
- 19
- 20
- 21
- 22
- 23
- 24
- 25
- 26
- 27
- 28
- 29
- 30
- 31
- 32
- 33
- 34
- 35
- 36
- 37
- 38
- 39
- 40
- 41
- 42
- 43
- 44
- 45
- 46
- 47
- 48
- 49
- 50
- 51
- 52
- 53
- 54
- 55
- 56
- 57
- 58
- 59
- 60
- 61
- 62
- 63
- 64
- 65

1501 Table 3. List of Machine Learning software libraries and their languages

1502

Libraries ML/DL	Source	Language
MICE, rpart, Party, CARET, randomForest, nnet, e1071, KernLab, igrph, glmnet, ROCR, tree, Rweka, earth, klaR,	https://cran.r-project.org/	R
Scikit-learn Tensorflow Theano Pylearn2, NuPIC Caffe PyBrain	http://scikit-learn.org/stable/ https://www.tensorflow.org/ http://deeplearning.net/software/theano http://deeplearning.net/software/pylearn2 http://numenta.org/ http://caffe.berkeleyvision.org/ http://pybrain.org/	Python
Weka Spark Mallet JSAT ELKI Java-ML	http://www.cs.waikato.ac.nz/ml/weka/ http://spark.apache.org/ http://mallet.cs.umass.edu/ https://github.com/EdwardRaff/JSAT http://elki.dbs.ifi.lmu.de/ http://java-ml.sourceforge.net/	Java
Accord Multiboost Shogun LibSVM mlpack Shark MLC++	http://accord-framework.net/ http://www.multiboost.org/ http://shogun-toolbox.org/ http://www.csie.ntu.edu.tw/~cjlin/libsvm/ http://mlpack.org/ http://image.diku.dk/shark/ http://www.sgi.com/tech/mlc/source.html	C#, C++, C

1503

1504

1505

1506

1507

1508 Table 4 A list of current procedures for image analysis based on the type of
 1509 sensor used.
 1510

Data type /Source	Pre-processing	Segmentation	Feature extraction	Machine Learning
Mono – RGB	<ul style="list-style-type: none"> * Homomorphic filtering to minimize illumination issues in outdoor images [199] * Filtering and histogram equalization in plant disease detection [136] 	<ul style="list-style-type: none"> * Many vegetation indexes apply to segmentation in [132] * NDVI index to discriminate background foreground [200] * Cellular neural networks edge detection [201] * HSV-algorithm [202] 	<ul style="list-style-type: none"> * Fourier descriptors and Zernike moments [201] * Statistical parameters and Wavelet transform with geometric characteristics [131] * SIFT and SURF in 3D reconstruction images from multiple RGB cameras with basil specimen [168] * Histogram to color features and Fast Fourier Transform + Discrete Wavelet Transform to texture features extraction [145] 	<ul style="list-style-type: none"> * ANN to detect Phalaenopsis seedling diseases [203] * SVM to detect tomatoes leaf viruses [204] * Gaussian mixture model to detect biotic stress in wheat [205] * k-NN to identify leaf disease [206] * Probabilistic Neural Networks and Genetic Algorithm [201] * Random forest to QTL analysis [207]
StereoVision	<ul style="list-style-type: none"> * Complete and general pre-processing pipeline [208] * Rectification of image based on SIFT and epipolar transformation, in vitis vinifera segmentation [209] * Camera stereo calibration, leaf quantifying Brassica napus [210] * RGB2GrayScale [211] * Align and depth estimation [212,213] 	<ul style="list-style-type: none"> * Otsu’s method & growing region [211] * SVM to remove background [213] 	<ul style="list-style-type: none"> * Graph-cut and local correlation [214] * SURF to stereo matching images base on theirs feature vectors [211] * Combined with thermal images (Global and local features (temperature, depth, color) using PCA and ANOVA [213] * Simple statistical and intensity values [212] 	<ul style="list-style-type: none"> * SVM identify diseased pixels in leaves [213] * SVM & Gaussian Processes Classifier (GPC) to detect soil moisture deficit [212]
Multi-Hyper spectral	<ul style="list-style-type: none"> * Savitzky-Golay filter: remove noise and smooth the image. [215] * Gaussian filter to 	<ul style="list-style-type: none"> * NDVI (750-705/750+705) nm with threshold of 0.20 [218] 	<ul style="list-style-type: none"> * Pixels averaged to obtain average reflectance [218] 	<ul style="list-style-type: none"> * Cascade of data mining techniques to detect foliar disease in barley leaves [219]

1
2
3
4
5
6
7
8
9
10
11
12
13
14
15
16
17
18
19
20
21
22
23
24
25
26
27
28
29
30
31
32
33
34
35
36
37
38
39
40
41
42
43
44
45
46
47
48
49
50
51
52
53
54
55
56
57
58
59
60
61
62
63
64
65

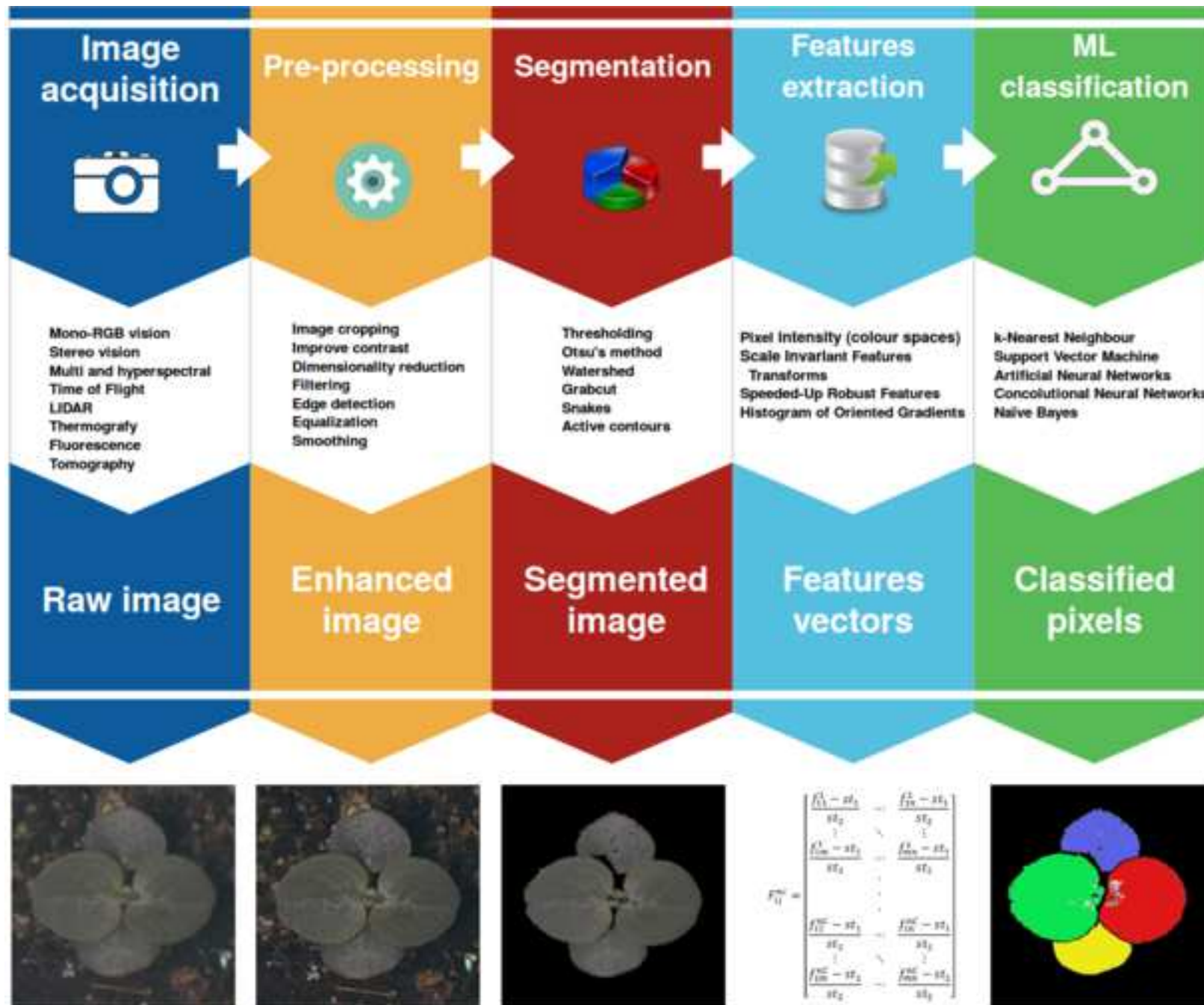
	<p>remove noise: detection of disease in banana leaves [216]</p> <p>* Savitzky-Golay filter: detection of disease in plants [217]</p>			<p>* Bayes, logistic, random forest and decision trees to detect biotic stress in <i>Alternaria</i> genus [173]</p> <p>* k-NN to identify leaf disease [206]</p> <p>* PCA and partial least squares regression to predict water, macro and micronutrients concentrations [218]</p>
ToF	<p>* Correction of the distance error caused by the extra contribution of electrons from sunlight using an offset parameter [68]</p> <p>* Carry-out a calibration stage before to fuse the depth data and color information [69,70]</p> <p>* Removal spurious individual points (outliers) using statistical filter [74]</p> <p>* Removal of lens distortion [220]</p>	<p>* Combine hierarchical color segmentation with quadratic surface fitting using ToF depth data [70]</p> <p>* The maximally stable extremal regions algorithm for the segmentation of single object over background in gray level images [221]</p> <p>* Removal background by simple thresholding pixel values greater than a certain threshold [220]</p> <p>* Segmentation inspired from the maximally stable extremal regions algorithm [221]</p>	<p>* SIFT, Hough Transform and RANSAC algorithm to extract relevant features [220]</p>	
LIDAR	<p>* RANSAC algorithm to detect ground plane [222]</p> <p>* Reduction of noise, filtering points clouds based on deviation [223]</p>	<p>* Clustering to detect individual plants [222]</p>	<p>* Statistical features from reflectance and geometry [222]</p> <p>* Surface feature histograms to characterize the grapevine and wheat organs [224]</p>	<p>* ANN for wheat green area index measurement [225]</p> <p>* ANN, SVM, logistic regression to plant identification (the best results) [222]</p> <p>* Generalized linear model (the best) to model plant richness [226]</p> <p>* SVM obtained</p>

1
2
3
4
5
6
7
8
9
10
11
12
13
14
15
16
17
18
19
20
21
22
23
24
25
26
27
28
29
30
31
32
33
34
35
36
37
38
39
40
41
42
43
44
45
46
47
48
49
50
51
52
53
54
55
56
57
58
59
60
61
62
63
64
65

				highly reliable classification about 96% [224]
Thermography / Flourescence	<ul style="list-style-type: none"> *Align with stereo images (In combination with stereo images) [212,213] * Normalize thermal information with thermal indexes [227] * Trimming extraneous images from image stack [228] 	<ul style="list-style-type: none"> * Semi automated segmentation through a geometric algorithm implemented in Python-based software ChopIt [228] * Manual thresholding comparing conventional color images with fluorescences images (Fv/Fm) [229] 	<ul style="list-style-type: none"> * Combined with thermal images (Global and local features: temperature, depth, color) using PCA and ANOVA [213] 	<ul style="list-style-type: none"> * SVM identify diseased pixels in leaves [213] * SVM and Gaussian Processes Classifier (GPC) to detect soil moisture deficit [212] * ANOVA (not ML) to analyze different water status [227] * ANN and SVM to detect zinc-deficiency stress using fluorescence imaging [230]
MRI/ Tomography	<ul style="list-style-type: none"> * 2D and 3D Fourier transformations (MRI) [231] * Median filter, binaryzation, fill holes, remove small particle and morphological filter (erosion) [232] * Re-slicing, cropping and contrast enhancement [233] 	<ul style="list-style-type: none"> * Yang2011: watershed segmentation [232] * Histogram thresholding method to binaryze the image [233] 	<ul style="list-style-type: none"> * Intensity features, Haralick textural features, intensity local binary pattern features, contrast features and Gabor intensity textural features [233] 	<ul style="list-style-type: none"> * Supervised learning with ANN, Mahalanobis distance, Linear discriminant analysis and quadratic discriminant analysis to determine boundary lines [233]

1511
1512
1513

1514		
1	1515	Figure Legends
2		
3	1516	
4	1517	
5		
6	1518	
7		
8	1519	Figure 1. Basic workflow in computer vision-based plant phenotyping
9		
10	1520	Figure 2. An overview of different spectra used for phenotyping and the associated
11	1521	cameras. Names of different indexes are found in Table 2.
12		
13	1522	
14		
15		
16		
17		
18		
19		
20		
21		
22		
23		
24		
25		
26		
27		
28		
29		
30		
31		
32		
33		
34		
35		
36		
37		
38		
39		
40		
41		
42		
43		
44		
45		
46		
47		
48		
49		
50		
51		
52		
53		
54		
55		
56		
57		
58		
59		
60		
61		
62		
63		
64		
65		



Text

Figure 2

